

Response to reviewers and manuscript with tracked changes for “Information content of OCO-2 oxygen A-band channels for retrieving marine liquid cloud properties”

Mark Richardson and Graeme L. Stephens

5 We have substantially modified our paper in response to reviewer comments. The Introduction has been lengthened and explains how past work suggested that OCO-2’s spectral resolution is sufficient to obtain cloud geometric thickness, whereas other instruments (e.g. SCIAMACHY, GOME) were not able to. We also explain how our approach is complementary to multi-angular measurements (e.g. POLDER, MSPI, 3MI) which contain information for physically thicker clouds, and discuss other modern instruments with similar spectral resolution (TROPOMI on Sentinel-5P and the spectrometers on GOSAT & the
10 FengYun-3 series).

Our new Figure 6 shows an OCO-2 cloudy scene spectrum with our selected micro-window to help readers contextualise our results, as suggested particularly by reviewer 1, but which addresses issues raised by other reviewers. This figure also includes an example GOME-2-like sampling of the same spectrum and reports the degrees of freedom for signal, showing that OCO-2 contains information on geometric thickness whereas the GOME-2-like signal does not. This fits with our

15 As suggested by reviewer 3, we have added degrees of freedom for signal to our information content analysis and show it on the relevant figures. This does not change any of the conclusions but eases interpretation for many readers.

A limitation of our work that was not adequately emphasised in the initial submission is overlying aerosol. We now discuss this in more detail in the text, but have not been able to implement proper aerosol-over-cloud calculations, this is under development now.

20 We believe that we have responded sufficiently to all reviewer comments and have made changes where necessary. With the link from the new introductory text to the degrees of freedom for OCO-2 versus GOME-2 example, we have a clear explanation of why our retrieval is new and adds to currently available products. We are thankful to the editor and reviewers for their time and attention, which has led to a greatly improved paper.

25 Contents:

1.....	Introduction
2.....	Response to reviewer 1
9.....	Response to reviewer 2
12.....	Response to reviewer 3
15.....	Response to reviewer 4
20.....	Manuscript with tracked changes

General response to reviewer 1

We have responded to each of your points below, with your text in red and ours in blue and believe we have addressed your major concerns. We did not act on some of your minor suggestions but have justified this in each case. Typically this is because of linguistic style choices or because of the AMTD template.

The largest changes made in response to your comments are that the introduction has been greatly extended and we have added a new Figure 6. This contains an example OCO-2 spectrum, highlights our micro-window and also shows a GOME-2-like spectrum. These make the paper much more accessible and allow much easier comparison with other instruments.

It is obvious that you read our submission with great attention, thank you for your time and feedback.

NOTE: our page and line numbers refer to the new version of the manuscript without tracked changes. With our greatly expanded introduction and other minor corrections it became very messy otherwise.

Detailed review on the paper: Information content of OCO-2 oxygen

A-band channels for retrieving marine liquid cloud properties.

I. General comments

I think this paper is very interesting and brings innovation on how to retrieve cloud properties with OCO-2. The use of optimal estimation method makes the study very robust.

I have some remarks concerning the introduction. I think you should rework it to make it more complete. Indeed you should answer the following questions:

- What are the motivations for this study?
- What has already been done?
- What does your study bring?

As those aspects are not clear. I also find your bibliography too light. We don't expect you to quote all the works done in the O2 A-band and optimal estimation, but at least some of them. You can read the paper of Merlin et al (2017) as the subject is close to yours and the bibliography is quite complete.

→ **Response:** We tried to keep the paper concise, but now agree that we missed too much context so have made major changes.

→ **Changes made:** Much rewritten and added text, covering p1L18—p3L34. The introduction has been rewritten and lengthened with citations to Hanel (1961), Yamamoto & Wark (1961), Deschamps et al. (1994), Ferlay et al. (2010), Desmons et al. (2013), Merlin et al. (2016), Yang et al. (2013), Rozanov & Kokhanovsky (2004), Schuessler et al. (2014), Heidinger & Stephens (2000) and O'Brien & Mitchell (1992). These support a new summary of various A-band cloud studies and then justify our new work as applying hyperspectral approaches that are useful for low clouds. We cite Bony & Dufresne (2005) and Zelinka et al. (2012) to support the importance of low clouds that are poorly sampled by the multi-angular approaches, and explain our advantages for geometrical thickness relative to other work that used instruments with lower SNR and spectral resolution.

II. Specific comments

p1

L 19-20, there are numerous papers that you can quote.

- **Response:** See changes above.
- **Changes made:** Introduction fully rewritten.

5 p2
I25: multiply scatter : not nice

- **Response:** Term deleted, the lidar being attenuated justifies the point on its own.
- **Changes made:** "...attenuate and multiply scatter the CALIPSO lidar" → "attenuate the CALIPSO lidar"

10 I25-26-27-28: This sentence is too long

- **Response:** Agreed.
- **Changes made:** Sentence split into two.

15 I31: This work: Sentence not clear

- **Response:** Justification added.
- **Changes made:** Sentence now reads: "Since any footprint that is identified as possibly cloudy is not processed in the standard OCO-2 products this work generates value from largely unused soundings."

20 p3
I4: do contain information.... Reference is missing

- **Response:** This is based on Nakajima-King-like principles but I don't have the formal information content analysis for the OCO-2 instrument. Therefore we changed the wording slightly and added a citation.
- **Changes made:** p4L22—25 changed and now reads "The CO₂ bands are not considered in this analysis but do inform about cloud phase and droplet or particle size (Nakajima and King, 1990), and this information will be used when this retrieval is applied in our observation-based study to identify likely liquid cloud cases."

30 I21 ECMWF meteorological fields : Reference missing

- **Response:**
- **Changes made:** p5L10—11 added text: "response as described in the OCO-2 data version 6 documentation (Boesch et al., 2015)"

35 p4
I18 observed and expected y : is a value missing after "observed"?

- **Response:** The meaning is intended as "observed y and expected y" but that feels clunky to me. Another option is to hyphenate to "observed- and expected y", but grammar guides now disagree over that use and it seems archaic. I thought context made it clear, but have added a little extra text to further emphasise the context.
- **Changes made:** p6L14—15 rewritten slightly to: "based on the difference between the observed and expected y"

45 I15 to 30: When you refer to a vector or a value you could write its symbol

- **Response:** Symbols added to aid the reader, with minor rephrasing so that it's clear that \hat{S} refers to the posterior uncertainty and not the "reduction in posterior uncertainty".
- **Changes made:** Vector and matrix symbols added and text changed, e.g. "reduction in posterior uncertainty" → "posterior uncertainty \hat{S} is reduced by..."

50

I22 observation vector instead of observation state vector

- **Response:**
- **Changes made:** change made.

5

I22 a point is missing after channels

- **Response:**
- **Changes made:** change made.

10

I27 Shannon entropy : Reference missing

- **Response:**
- **Changes made:** p6L30 now reads "...and this change in associated Shannon entropy (Shannon and Weaver, 1949)..."

15

p5
I1: You don't define P0 and P1

20

- **Response:**
- **Changes made:** p7L2—4 now reads "In this case $S(P_0)$ is the Shannon entropy associated with the original probability distribution and $S(P_0)$ the same value associated with the retrieved probability distribution."

25

I6 :see my comment p4 I15

- **Response:**
- **Changes made:** Symbol added.

30

I19 : Methodology **and** example atmosphere **and** cloud ..
Not nice.

- **Response:**
- **Changes made:** Changed to "Methodology, atmospheric states and cloud cases"

35

p6
I1 pw not present in eq 8

40

- **Response:** Good catch, this was a typo.
- **Changes made:** ρ converted to ρ_w in Equation 8.

I7: Why do you take $Q_{ext} = 2$?

45

- **Response:** Size parameters $x = 2\pi r/\lambda$ here are >50 and water is weakly absorbing (real part of index ~ 1.33 , imaginary part $\sim 1 \times 10^{-7}$), so I take $\lim_{x \rightarrow \infty}$ case for a non-absorbing sphere.
- **Changes made:** p8L6—7 text added: "This value is chosen as it represents the large-particle limit for non-absorbing spheres (Herman, 1962) which is a reasonable approximation for cloud droplets in the oxygen A-band"

50

I7: 0° - 20° , 20° - 50° and 50° - 90° , you forgot the degree symbol over 0, 20 and 50.

→ **Response:** This appears to be an AMT style choice. Under “English guidelines and house standards” it says “En dashes (–) are longer than hyphens (-) and serve numerous purposes...En dashes are used to indicate, among other things, relationships (e.g. ocean–atmosphere exchange), ranges (e.g. 12–20 months),...” this implies that for ranges the unit follows the latter value only.

5 → **Changes made:** None

I7: 'identified as single-layer liquid clouds by both MODIS and CaLiPSO'. It may be useful for the reader to write which product/ collection you used.

10 → **Response:**

→ **Changes made:** p8L14—15 now reads: “The MODIS data are from product MYD06 at 1 km horizontal resolution (Platnick et al., 2015) and the CALIPSO data are from the 1 km resolution cloud layer product 01kmCLay (Vaughan et al., 2009).”

15 I8-9: You should rewrite the 2 sentences which are not clear. For instance :

'Within each bin, all the OCO-2 ECMWF-Aux profiles (including pressure, temperature, humidity and wind speed) are averaged level by level.'

20 → **Response:** Agreed.

→ **Changes made:** p8L15—17 now use your suggested text.

I22: not nice. You should rewrite the description of the uncertainties, particularly for the humidity.

25 → **Response:** The humidity method description was split by the temperature sampling description, we've rewritten to ensure that the specific humidity perturbations are described continuously and hope that this is clearer.

30 → **Changes made:** p8L30—p9L2 now reads: “For temperature we add a uniform perturbation to each level with a value sampled from a zero mean (μ) Gaussian with standard deviation (σ) of ± 1.5 K. For specific humidity we sample from a zero mean Gaussian with a standard deviation of unity, then scale this value based on pressure level. The scaling is equivalent to ± 20 % of the initial specific humidity at the surface, increasing linearly to ± 50 % of the layer values at 250 hPa and remaining at ± 50 % for levels with lower pressure.”

35 I25: standard deviation of ± 1.5 K
we sample: what are you sampling?

40 → **Response:** Above text change hopefully addresses this.

→ **Changes made:** See above.

I26: with 2000 perturbations **applied** to reff

45 → **Response.**

→ **Changes made:** “applied” added.

I27: '5--95% range of 7.5--19.4 μm ' Not sure of what it means. Try to avoid the abbreviations in the text and write a sentence.

50 → **Response:** We have rewritten this in a way that we hope is clearer.

→ **Changes made:** p9L4—5 now reads: “This lognormal fit has an arithmetic mean of 12.0 μm , but after excluding values outside the 4—30 μm retrieved by MODIS, the arithmetic mean is 12.6 μm and 5—95 % of the values fall within 7.5—19.4 μm .”

I29: The output was **sampled**: You are using this word quite often and maybe not always with the right sense?

→ **Response:** Agreed.

→ **Changes made:** p9L12—13 now reads: " The output spectra are calculated for each of the 8 different instrument line shapes associated with the 8 different OCO-2 across-track sounding positions"

p7

I8: cases **described** in sect. 3.1

→ **Response:** Agreed

→ **Changes made:** "described" inserted.

I12: not nice: to an error of 1.5 on τ , of 60hPa on Ptop and of 7.5hPa on ΔP

→ **Response:**

→ **Changes made:** suggested text changes made.

I14: Our uncertainty is approximately: What does it mean?

→ **Response:** This refers to some results from Richardson et al. (2017), we have rephrased.

→ **Changes made:** p9L29—32 now reads: "Our τ prior error comes from applying the $\pm 18\%$ error in simulated radiance for homogeneous clouds when provided with MODIS optical depth (Richardson et al., 2017). Our Ptop uncertainty is from the standard deviation of the differences between OCO-2 and CALIPSO P_top when using a simple lookup table for OCO-2, which we intend to use for the OCO-2 prior. The ΔP uncertainty is similar to the $\pm 20\%$ error associated with Eq. (8) for clouds of cloud fraction > 0.8 reported in (Bennartz, 2007)."

I18-19: 'more intuitive': not very nice, more qualitative ?

→ **Response:** We feel that either option is ok, but I don't know how to calculate "quantitative-ness" of using the square root of an element of a covariance matrix versus information content. However, we think that most readers will find values expressed in optical depth units or hPa to be more intuitive than information content in bits so prefer to keep the current phrasing.

→ **Changes made:** None

p9

Description of figure 3: I am confused as the caption seems to say that there are two figures (top and bottom), but only one is visible. Description of figure 4: I don't know where to see the channels you are mentioning (I9) as the plot is in function of the OCO-pixels. It might be a good idea to show a spectra of OCO lines.

→ **Response:** Figure 3 was changed just prior to submission and caption was not, we've fixed it. Our new Figure 6 contains an OCO-2 spectrum along with an approximated GOME-2 spectrum of the same scene after determining the micro-window to use and calculating information metrics. We show it this late in the paper since showing it before the IC calculations and micro-window selection might confuse readers. To help further we changed the x coordinates of Figure 4 to wavelength and then presenting a spectrum later would be sufficient for readers to follow. The inclusion of a GOME-2-like spectrum and calculation is to help readers understand the extra value of OCO-2's high spectral resolution. This addresses various reviewer comments, including your first one about what value we add and how we compare with previous work.

→ **Changes made:** Figure 3 caption rewritten, keeping single figure. Figure 4 xlabel changed to wavelength units. New Figure 6 is an example spectrum with the 75 channel micro-window highlighted, a GOME-2 equivalent spectrum and the degrees of freedom for signal added to the legend.

Description of figure 5:
I20 content2. remove the 2.

- 5
- **Response:** Good spot, thanks.
 - **Changes made:** Deleted the 2.

I23: Again showing a spectra with your selected window might be a good idea.

- 10
- **Response:**
 - **Changes made:** See previously, spectrum added in Figure 6.

15 Also How did you choose the thresholds? You should justify more the choice of 75p as it is not obvious from the plot. 50p could be fine also?

- 20
- **Response:** We have edited the text to emphasise that we also aimed to consistently satisfy the P_{top} and ΔP_c criteria as well. The addition of the degrees of freedom for signal to our analysis should also help clarify things.
 - **Changes made:** p12L16—20 now reads: “The median case in the 50 channel micro-window passes our IC threshold and in all cases passes the τ -uncertainty threshold, but it has multiple cases that fail the P_{top} and ΔP_c thresholds. By contrast, the 75 channel micro-window containing the OCO-2 channels 353—426 (indices counting from 1 for the full 1,016 OCO-2 L1bSc channels) consistently satisfies our P_{top} and ΔP_c criteria and reduces the full wavelength range from 759.2—771.8 nm to 763.5—764.6 nm.”

25 p10
I2-3: Once again, showing a spectra would help the reader to follow your conclusions.

- 30
- **Response:**
 - **Changes made:** See previously, Figure 6 displays spectrum.

I9-10-11: Sentence too long.

- 35
- **Response:**
 - **Changes made:** Sentence broken into two. Similar changes to nearby sentences.

III. Technical corrections

40 When you quote a paper within a sentence (p2 I3) you shouldn't put the author's name between parentheses. This study goes beyond Richardson et al (2017) by

- 45
- **Response:** This is a reference manager issue.
 - **Changes made:** Sentence rewritten to avoid parentheses. We will ensure that, if the paper is accepted, we parentheses throughout will be properly handled.

I don't know what is the AMT policy for that but it would be better to centre your equations.

- 50
- **Response:** We're using the template, it seems AMT formatting changes this.
 - **Changes made:** None now, will use AMT format if accepted.

In the bibliography, you might think to put the first authors in bold and the titles in Italic; otherwise it is very difficult to distinguish the different papers.

→ **Response:** We used a reference manager plugin with the template, it seems that, if accepted, AMT has a different format to AMTD which will fix this.

→ **Changes made:** None now, will use AMT format if accepted.

5 **Figures:** In general, be careful with the size of the axis-labels which are very small (fig 2 , 4)

→ **Response:** Agreed. If accepted we will keep an eye on this make sure that resizing figures doesn't make the text too small.

→ **Changes made:** Axis label fontsize default increased.

10

The numbers of the lines restart at 0 at each page, I don't know if it is a mistake or not.

→ **Response:** We re-downloaded the AMTD template and found the same, it appears to be a template choice.

→ **Changes made:** None.

15

20

25

30

General response to reviewer 2

We have responded to each of your points below, with your text in red and ours in blue.

5 Firstly, we haven't specifically mentioned airborne data, although some of our citations and text now refer to instruments that have airborne versions (e.g. MSP1). We're definitely interested in seeing the outcome of more airborne campaigns and comparing our functioning retrieval with available airborne data including non-A-band sensors. A next step is to look at ORACLES data to assist with our validation since they have some flights designed to underpass CloudsSat, which has the same reference ground track as OCO-2

10 The ORACLES example brings us neatly to the issue of aerosols: our current radiative transfer implementation has had some problems with adding above cloud aerosol. We have plans to transfer the code to optimise for scattering atmospheres but we believe that sufficient caveats mean that this paper is still justified (after all, other recent cloudy information content papers have worked on single layer cloudy scenes too!). We have added text and citations regarding aerosols and highlight that it is a source of uncertainty that we must address.

15 Your suggestion of using the multi-layer mask from MODIS is excellent and we are considering and testing it now. We are currently running our retrieval with CALIPSO priors as well, but MODIS has the advantage of a longer expected time in the A-train. Ultimately we would like to identify multi-layer cases with OCO instrumentation alone so that our retrieval could be applied to e.g. potential OCO-3 measurements even if no other MODIS-like or CATS-like instruments are available to identify multi-layer cases. However, CloudSat-CALIPSO and MODIS multi-layer data are vital to allow us to develop and test this technique.

Thanks for taking the time to review our paper, you spotted several unclear points or typos that we have now fixed.

25 **NOTE:** our page and line numbers refer to the new version of the manuscript without tracked changes. With our greatly expanded introduction and other minor corrections it became very messy otherwise.

Review of Richardson & Stephens paper:

30 This is a very interesting and valuable study. I would be very interested to know how this study could transfer to airborne spectrometers like AVIRIS and PICARD that also have high spectral resolution and lack IR channels for cloud top retrieval. We've done a similar thing with ASTER: used an instrument that was previously only for clear-sky work and created a product from unused data. The paper is overall well written and methods are clearly described and understandable.

Major comments:

35 Marine SCu frequently have some kind of aerosol sitting on top of them especially off the coast of Africa (Sahara dust and Namibia smoke) and to a lesser extent the US Pacific Coast (mostly smoke). Have you tried inserting above-cloud aerosol layers into your simulations and seeing what happens? I'm not saying that you have to correct for aerosols but some idea as to uncertainty introduced by absorbing aerosols would be nice.

40 → **Response:** We have added some discussion about aerosols and indicated that we do not consider them in this study. There have been some technical problems implementing aerosol layers into our modified cloudy-scene radiative transfer model. Much other A-band work has considered clear-sky cases and we have discussed the prevalence of aerosol in the new text, and note that we should be able to flag heavily polluted cases using collocated data. Future work will look in more detail at overlying aerosol, and speculatively I expect an effect on the residual spectral fits from the retrieval which may allow identification based on OCO-2 alone.

→ **Changes made:** p3L10—12 now reads: “Our current analysis considers aerosol-free cases as aerosols have not yet been properly implemented in our modified cloudy-sky version of the radiative transfer model, this is an avenue for future work and will be discussed in Sect. 5.”

5 P13L32—p14L9 now reads: “Alternatively, since OCO-2 flies in the A-train it would also be possible to use other sensors such as CALIPSO (which is now leaving the A-train) or MODIS to identify multi-layer cloud cases, or scenes in which there is heavy aerosol loading. Cases of heavy aerosol loading are most common over the Namibian stratocumulus region with common occurrence in June-July-August (JJA) and a peak in September-October-November (SON). A combination of CALIPSO, CloudSat and International Satellite Cloud Climatology Project (ISCCP) data imply that in the SON Namibian stratocumulus region, approximately one-third of low clouds have overlying aerosol, and approximately half of these cases are smoke (Devasthale and Thomas, 2011; Winker et al., 2010). Scattering layers overlying a marine cloud tend to reduce in the effective retrieved cloud layer pressure due to the reduced mean path length of those photons reflected from the overlying layer (Vanbauce et al., 1998). Assessment of aerosol effects will be necessary in future work.”

15
Please be consistent in definition of micro-window. You use “pixels” in the first 8.5 pages of the paper and then switch to “channels” for the rest of the text. I personally would prefer you use “channels”, but you can use whichever you see fit as long as it’s consistent throughout.

- 20 → **Response:** Agreed, this was a legacy from our use in a previous paper and some OCO-2 documentation but is confusing.
→ **Changes made:** We now use the correct term “focal plane array elements” when discussing damage to the sensor, and “channels” for all spectral properties.

25 **Minor comments:**

Figure 3 caption should read $\mu_{0-2}=\cos^{-2}(\text{SZA})$, μ is normally used to indicate sensor zenith angle.

- 30 → **Response:** Oops.
→ **Changes made:** Labels changed throughout, $\mu \rightarrow \mu_0$

Page 1 Line 1: please expand CALIPSO acronym, first use

- 35 → **Response:** Done.
→ **Changes made:** CALIPSO is now introduced on p2L13 following our major changes to the introduction, its acronym is expanded.

Page 2 Line 21: should read “equator crossing time near 13:30”

- 40 → **Response:**
→ **Changes made:** Done.

Page 7 Line 25: please clarify what the micro-windows are measured in: 500 of what? Later in the text, on page 9 it becomes clear that the units of the micro-window size are channels. For folks that don’t normally use something like OCO, it might help giving a bit more information, like what a 75-channel micro-window translates into as far as a wavelength range goes. It would make the research more transferable to other instruments as this is a potentially very valuable retrieval approach.

→ **Response:** This was unclear on our part. We have now clarified throughout, adding “channels” after 500. The 75 channel wavelength range is given. The new Figure 6, made in response to reviewer 1, also hopefully clarifies things.

5

→ **Changes made:** p10L9—10 now reads: “To make this problem tractable, we select micro-windows of the following size: 5, 10, 25, 50, 75, 100, 150, 200 and 500 neighbouring channels.” (note added word “channels”)

p12L17—28 text includes: “By contrast, the 75 channel micro-window...reduces the full wavelength range from 759.2—771.8 nm to 763.5—764.6 nm.”

10

Figure 6 added to visualise this.

Page 9 Line 3: please use θ_0 and μ_0 as is generally customary for solar zenith angle and its cosine

→ **Response:** Agreed.

15

→ **Changes made:** Done.

Page 9 Line 20: “highest mean information content2. “ A typo?

→ **Response:** Good catch.

20

→ **Changes made:** 2 deleted.

Page 10 Line 26: OCO is in the constellation with Aqua, so you may be able to use the MODIS multilayer cloud map in order to stay away from cirrus. That’s just what that map is for.

25

→ **Response:** We have done some preliminary analysis using this for validation of the retrieval and it makes a difference (same as multiple layers from CALIPSO). This was helpful in our discussion, thanks.

→ **Changes made:** See aerosol response text, we now mention the multi-layer map.

30

35

General response to reviewer 3

We have responded to each of your points below, with your text in red and ours in blue. We have made changes to address all of your technical comments. After playing around with the organisation and ordering of the text, we decided to keep the current structure but change section titles to help readers follow.

5

We have found that we get pretty good match with the MODIS cloud flag by using a simple brightness threshold, and similarly get a good match (~93 % agreement) on cloud phase using a simple derived Nakajima-King diagram. Our retrieval is now running through the OCO-2 data record but we haven't finalised thresholds for warning levels etc. For SZA < 60° We can match when MODIS is confidently cloudy in 93—96 % of cases depending on the orbit, for a set of test orbits we have done. We can also increase the thresholds to do fewer retrievals, but be more likely to retrieve when MODIS also obtains cloud properties (the numbers differ since MODIS retrieval does not provide e.g. τ for every confidently cloudy scene).

10

We feel that adding these preliminary results would clutter the paper and the thresholds may change before product release so have just expanded the discussion to address your points.

15

Your suggestion of adding degrees of freedom for signal and adding a comparison versus lower spectral resolution results has clearly improved the paper. Fortunately we easily replicated the Schuessler et al. GOME-2 results and they fit very neatly into the narrative in our introduction.

20

Thanks for your time and helpful review.

NOTE: our page and line numbers refer to the new version of the manuscript without tracked changes. With our greatly expanded introduction and other minor corrections it became very messy otherwise.

25

Interactive comment on “Information content of OCO-2 oxygen A-band channels for retrieving marine liquid cloud properties” by Mark Richardson and Graeme L. Stephens

30

Anonymous Referee #3

Received and published: 24 October 2017

Review comments on manuscript “Information content of OCO-2 oxygen A-band channels for retrieving marine liquid cloud properties”

35

Authors: M. Richardson and G. L. Stephens

MS No.: amt-2017-314

40

MS Type: Research article

General comments:

This paper presents a theoretical study on retrieving marine boundary layer cloud optical thickness, pressure thickness, and top pressure, using the OCO-2 oxygen A-band measurements. The method is well defined and the results are of interests to the community. The topic is suitable for publication in AMT, but I do have some concerns for the authors to consider.

45

1) Marine boundary layer clouds are targets that we have pretty good a priori knowledge; hence it's not surprising to have good retrieval accuracy, but since the goal of the research is to apply the method to OCO-2 retrievals, one question would

50

be how to decide when to retrieve? I would suggest adding at least some discussions on how to identify the clouds that are suitable for applying this method.

5 → **Response:** We are preparing a paper and Algorithm Theoretical Basis Document to explain our full implementation in practice and didn't want to clutter this paper. However, we understand that readers may be interested in some of the general principles we will apply so have made the changes listed below. Some further justification: the OCO-2 preprocessors provide cloud flags, but they are optimised for glint only over ocean (e.g. Taylor et al. 2016, cited in the text for its collocated data) and we found we could not use it in nadir. Instead, we use a simple brightness threshold after accounting for solar zenith angle. Initial tests show >90 % agreement with MODIS cloud flags, depending on the orbit.

10 → **Changes made:** Text added to discussion: "Cloud identification is relatively simple for nadir A-band reflectance measurements over ocean, as for most solar zenith angles the surface is dark and cloudy scenes may simply be identified when reflectance exceeds some threshold, which depends on the viewing geometry".

15 2) The literature review should have been more complete. There have been studies on retrieving cloud pressure thickness plus cloud top pressure in the past, especially for thick clouds over dark surfaces (e.g., Ferlay et al. 2010, Yang et al. 2013, Merlin et al., 2016, reference given below).

→ **Response:** Agreed, the introduction has been changed.

20 → **Changes made:** The introduction has been rewritten and substantially lengthened with citations to Hanel (1961), Yamamoto & Wark (1961), Deschamps et al. (1994), Ferlay et al. (2010), Desmons et al. (2013), Merlin et al. (2016), Yang et al. (2013), Rozanov & Kokhanovsky (2004), Schuessler et al. (2014), Heidinger & Stephens (2000) and O'Brien & Mitchell (1992). These support a new summary of various A-band cloud studies and then justify our new work as applying hyperspectral approaches that are useful for low clouds. We cite Bony & Dufresne (2005) and Zelinka et al. (2012) to support the importance of low clouds that are poorly sampled by the multi-angular approaches, and explain our advantages for geometrical thickness relative to other work that used instruments with lower SNR and spectral resolution.

30 3) I found the structure of the paper makes understanding the contents difficult. I would suggest some re-arrangements. For example, Section 2 is titled "The OCO-2 satellite and its instruments", I couldn't see how the two subsections fit there: " 2.1 OCO-2 radiative transfer calculations" and "2.2 Optimal estimation and information content". My suggestion would be to use one section to describe forward modeling issues and another section for retrieval related issues.

35 → **Response:** We looked into moving things around but decided that we prefer the current organisation, but agree that the titles are confusing. Our separation is (Section 2) general information and techniques introduced and (Section 3) Specific techniques and samples used in this paper. Going for (Optimal Estimation) followed by or leading (Forward model) also seemed somewhat confusing given it leaves no obvious place to put the synthetic retrievals, and aspects needed for the optimal estimation (e.g. our sampling methodology) require understanding of the forward modelling and vice versa. We think that whichever way could confuse some readers, but think that after modifying Section 2 and 3 titles things are clearer this way.

40 → **Changes made:** Section 2 title changed to "Data sources and analysis techniques"

45 4) I would suggest converting the information content shown in the article to how many pieces of information can be retrieved. For example, it's not clear to me what information content = 16 means (the red line in Figure 4(a)) physically.

→ **Response:** We had thought that the low posterior errors were sufficient to indicate that the degrees of freedom or signal approached 3, but agree that there isn't actually that clear. We have therefore added d_s to our figures and discussion.

50 → **Changes made:** degrees of freedom for signal introduced in Section 3 along with the equation we use to calculate it. Figures 4 and 5 now have it, and legend of new Figure 6 includes example values.

References:

Ferlay, N., and F. Thieuleux, C. Cornet, and A. B. Davis, 2010: Toward New Inferences about Cloud Structures from Multidirectional Measurements in the Oxygen A Band: Middle-of-Cloud Pressure and Cloud Geometrical Thickness from POLDER-3/PARASOL. *J. Appl. Meteor. Climatol.*, 49, 2492–2507. doi: C2 <http://dx.doi.org/10.1175/2010JAMC2550.1>.

5 Merlin, G., Riedi, J., Labonnote, L. C., Cornet, C., Davis, A. B., Dubuisson, P., .Parol, F., 2016: Cloud information content analysis of multi-angular measurements in the oxygen A-band: Application to 3MI and MSPI. *Atmospheric Measurement Techniques*, 9(10), 4977-4995. doi:<http://dx.doi.org/10.5194/amt-9-4977-2016>.

10 Yang, Y., A. Marshak, J. Mao, A. Lyapustin, J. Herman, 2013: A Method of Retrieving Cloud Top Height and Cloud Geometrical Thickness with Oxygen A and B bands for the Deep Space Climate Observatory (DSCOVR) Mission: Radiative Transfer Simulations. *J. Quant. Spectrosc. Radiat. Trans.* 122, 141-149, <http://dx.doi.org/10.1016/j.jqsrt.2012.09.017>.

15

20

25

30

35

40

45

50

General response to reviewer 4

We have responded to each of your points below, with your text in red and ours in blue.

5 You identified a number of areas where we did not provide enough information for easy replication, and also a number of areas where we did not provide enough context or emphasise key points of interest for more general readers. Our changes have addressed all of your points and your incisive comments greatly improved the paper. Thank you for your time.

10 In some cases we struggled between clarity and providing details but have found a balance. For example, we use $12\ \mu\text{m}$ for r_{eff} based on the mean of the full PDF that is fit to MODIS data being $12.0\ \mu\text{m}$, but after applying thresholds the mean shifts to $12.6\ \mu\text{m}$, explaining some apparent differences in our original submission. We have added explanatory text where necessary.

15 Our updated introduction and Figure 6 combine to tell a nice story: OCO-2 has sufficient spectral resolution to retrieve geometric thickness, given our assumptions and based on previous work which we now describe in more detail. MERIS or even GOME-2 do not, and our new Figure 6 shows a GOME-2-like calculation where we replicate previous work by Schuessler et al. Multi-angular measurements should retrieve thickness, but only for geometrically thick clouds (multi-km+), so OCO-2 is complementary to them.

20 Other instruments have high spectral resolution so the results may carry over, and we list those of which we are aware (TROPOMI on Sentinel-5P, the spectrometers on the FengYun-3 series and GOSAT). We also point out where spatial resolutions differ (OCO-2 is better than TROPOMI/GOSAT), but also that OCO-2's narrow swath is a limitation compared with TROPOMI's much better coverage.

25 Changes made based on your comments, and those of the other reviewers, have made us provide much more context and resulted in a richer narrative that we hope will make the paper far easier to read and more widely useful. Thanks once again.

30 **NOTE:** our page and line numbers refer to the new version of the manuscript without tracked changes. With our greatly expanded introduction and other minor corrections it became very messy otherwise.

35 **Interactive comment on “Information content of OCO-2 oxygen A-band channels for retrieving marine liquid cloud properties” by Mark Richardson and Graeme L. Stephens**

Anonymous Referee #4

40 Received and published: 30 October 2017

This paper analyzed the information content in O2 A band for retrieving marine liquid cloud properties. it used the Rodgers (2000) formal optimization framework and expressed the information content in terms of degree of freedom for signal and Shannon entropy. The O2 A band on OCO-2 has 800+ channels, and this paper shows that only ~75 channels are needed to retain all information content for retrieving cloud optical depth, cloud pressure thickness, and cloud-top pressure. The method in this paper is sound, but revisions are needed to include various advances in recent studies of using O2 A and B for cloud/aerosol height retrievals, as well as more justification about assumptions and caveats in this study.

50

1. Abstract. what is cloud-pressure thickness? what is the unit here?

→ **Response:**

→ **Changes made:** Abstract changed: "...and cloud-pressure thickness, which is the geometric thickness expressed in hPa."

2. Introduction. Most references cited in the first paragraph are theoretic work done in the past. While they are interesting, there are renewed interests in recent years to use O2 A and B band to retrieve cloud/aerosol height, with some using real data with good validations. They should be included in this paper, and discussion should be made that recent studies with real data use only O2 A/B bands from an imager (such as EPIC or MERES), although some studies did recommend the use of spectra to retrieve aerosol height. See references below and references therein (including some work done by authors' colleagues in JPL).

Ding, S. et al., 2016, Polarimetric remote sensing in O2 A and B bands: Sensitivity study and information content analysis for vertical profile of aerosols, Atmospheric Measurement Techniques, 9, 2077-2092.

Xu, X. et al., 2017, Passive remote sensing of altitude and optical depth of dust plumes using the oxygen A and B bands: First results from EPIC/DSCOVR at Lagrange-1 point, Geophys. Res. Lett., 44, 7544-7554.

→ **Response:** We chose to be brief and limit discussion to things relevant to our hyperspectral result, but agree that we sliced out too much contextual work. Our changes were made to address all reviewers and we decided to focus on the cloud-relevant components. We reference Yang et al. (2013) for EPIC/DSCOVR since they looked at clouds. We add Ding et al. later in the text (see comment 5).

→ **Changes made:** The introduction has been rewritten and substantially lengthened with citations to Hanel (1961), Yamamoto & Wark (1961), Deschamps et al. (1994), Ferlay et al. (2010), Desmons et al. (2013), Merlin et al. (2016), Yang et al. (2013), Rozanov & Kokhanovsky (2004), Schuessler et al. (2014), Heidinger & Stephens (2000) and O'Brien & Mitchell (1992). These support a new summary of various A-band cloud studies and then justify our new work as applying hyperspectral approaches that are useful for low clouds. We cite Bony & Dufresne (2005) and Zelinka et al. (2012) to support the importance of low clouds that are poorly sampled by the multi-angular approaches, and explain our advantages for geometrical thickness relative to other work that used instruments with lower SNR and spectral resolution.

3. Section 2. It should be made clear if cloud properties are well characterized, will CO2 be retrieved accurately in cloudy-sky conditions? If so, is it column CO2 above cloud top or whole atmospheric column, including CO2 within cloud? Any references will be helpful in this regard. To what degree of accuracy of cloud properties are needed in order to retrieve CO2 with good accuracy?

→ **Response:** Our current retrieval will not allow this because we do not retrieve droplet effective radius, and droplet radius is needed since the wavelength differences between the O2 band and CO2 bands is large enough that it matters for the XCO2 retrieval. We now cite a paper whose figure shows that not knowing the droplet size causes a ~15 ppm spread in above-cloud CO2 retrievals, which is far larger than the <1 ppm that are reported as the requirements for the flux modellers.

→ **Changes made:** p3L30—p3L24 now reads: "This approach aims to optimise a cloud property retrieval and due to limitations related to the radiative transfer implementation and computational burden, droplet size is not a retrieved property but contributes to the posterior uncertainty. Above-cloud CO2 retrievals have been found to require cloud droplet size for good accuracy (Vidot et al., 2009) and therefore our current implementation will not directly lead to above-cloud CO2 retrievals."

4. Section 2.1. It is noted that there are often aerosol layer above marine boundary layer cloud. To be clear, no aerosol effects are treated in L2RTM, correct? How about surface reflectance?

→ **Response:** We have had some issues properly integrating aerosols into the cloudy-scene L2RTM, although the operational "clear sky" XCO2 retrieval run for the OCO-2 mission allows for optically thin layers of

stratospheric aerosols. We have added text to emphasise the limitations and that this is future work. We also realise that the surface requires further explanation. We now describe our surface model.

5 → **Changes made:** Regarding the surface, p3L32—p4L2 now reads: “Water surfaces at nadir are dark, and even in cloud-free cases there is rarely sufficient SNR for the OCO-2 algorithm to attempt an XCO₂ retrieval. We assume a Cox-Munk surface reflectance function with the L2RTM surface reflectance set to 0.10, but as we only use nadir view over ocean there is little sensitivity to surface properties.”

10 → Regarding aerosols, p3L10—12 now reads: “Our current analysis considers aerosol-free cases as aerosols have not yet been properly implemented in our modified cloudy-sky version of the radiative transfer model, this is an avenue for future work and will be discussed in Sect. 5.”

15 P13L32—p14L9 now reads: “Alternatively, since OCO-2 flies in the A-train it would also be possible to use other sensors such as CALIPSO (which is now leaving the A-train) or MODIS to identify multi-layer cloud cases, or scenes in which there is heavy aerosol loading. Cases of heavy aerosol loading are most common over the Namibian stratocumulus region with common occurrence in June-July-August (JJA) and a peak in September-October-November (SON). A combination of CALIPSO, CloudSat and International Satellite Cloud Climatology Project (ISCCP) data imply that in the SON Namibian stratocumulus region, approximately one-third of low clouds have overlying aerosol, and approximately half of these cases are smoke (Devasthale and Thomas, 2011; Winker et al., 2010). Scattering layers overlying a marine cloud tend to reduce in the effective retrieved cloud layer pressure due to the reduced mean path length of those photons reflected from the overlying layer (Vanbauce et al., 1998). Assessment of aerosol effects will be necessary in future work.”

25 section 2.2. what is the state vector? optical depth, top pressure/height? be clear here. This also applies to the title of this paper. what properties to be retrieved? droplet size, top pressure/height or optical depth?

30 → **Response:**

→ **Changes made:** p6L4—p6L6 now reads: “We follow the principles of optimal estimation from (Rodgers, 2000), where a Bayesian retrieval combines an observation vector y with a prior state vector x_a and obtains a posterior state x^* . In our case the state vector consists of cloud-top pressure P_{top} , cloud pressure thickness ΔP_c and cloud optical depth τ .”

35 5. Page 4, Line 25. Ding et al. (2016) used similar method to select channels needed in O₂ A and B band for aerosol retrievals. It is worthy to mention here.

40 → **Response:**

→ **Changes made:** Text added: “...(Chang et al., 2017; Mahfouf et al., 2015; Martinet et al., 2014; Rabier et al., 2002), and this approach has already been used in an oxygen A-band and B-band analysis for aerosol retrievals (Ding et al., 2016).”

6. Page 5, L20. How about effective variance of cloud droplet size? Does it matter?

45 → **Response:** See response to comment 8.

→ **Changes made:**

50 7. Page 6, L2. "A pressure scale height of 8 km is assumed to convert the resultant....". This sentence is hard to comprehend.

→ **Response:**

→ **Changes made:** text re-written as “Cloud geometric thickness is converted to pressure thickness by assuming that pressure decreases exponentially with altitude with a scale height of 8 km”

8. Page 6, L27. mean of 12.6 μm ? should it be 12 μm to be consistent with previously stated? How about effective variance?

→ **Response:** With our modified L2FP code we have to select integer values of r_{eff} and picked a value close to the peak (the exact value depends on the statistic you use: arithmetic mean is 12.6 microns but you can get other values from a log fit, taking the median, mode or others). We have mentioned the integer sampling earlier in the text, but think that adding extra text here is clunky so have made no changes. We have, however, added clarification text where we think it does not interrupt the flow.

→ **Changes made:** p5L29—p5L32 now reads: “Mie scattering computations are used within louds using relevant coefficients that are pre-calculated for gamma distributions of cloud droplets based on a summary of low-cloud studies (Miles et al., 2000). These values have only been pre-computed for integer values of effective droplet size. This should not affect our results greatly since our calculated uncertainties include a term spanning a range of droplet sizes.”

P11L4—o117 now reads: “The r_{eff} distribution effective variance is fixed in each case in order to use the pre-calculated scattering properties used with the L2RTM code, but given the wide range of effective mean values considered, it is not expected that allowing the effective variance to change would greatly affect the results.”

9. Page 6, L29. cloud top pressure of 850 hpa? but, in the 3.1, it says three different pressures.

→ **Response:** We calculated covariance calculations for a single cloud-top pressure but used multiple cloud-top pressures in the calculation of information content and in the synthetic retrievals to more effectively use compute time. Our posterior sample spread from the synthetic retrievals therefore includes any uncertainty introduced by calculating the covariances at a single ctP .

→ **Changes made:** p9L9—p9L11 now reads: “. We calculate covariances at a single value of P_{top} , but the convergence of our synthetic retrieval tests across a range of true P_{top} values shows that we obtain reliable results regardless.”

10. Page 8, L10. what is the priori for cloud top pressure here? what is the error in OCO-2 measurement itself?

→ **Response:** Clarification text added. We had provided information on the P_{top} apriori but not the specific instrumental uncertainty relevant to these values. We have repeated the P_{top} prior details so that hopefully readers don't miss them.

→ **Changes made:** p10L25—p11L2 now reads: “The squared OCO-2 radiance uncertainties are added to the diagonal elements of the observation error covariance matrix with no cross correlation. We use the standard OCO-2 version 7 uncertainties, and SNR increases as the radiance in a given channel increases. The median SNR ranges from just over 400 for the $\tau = 5$ cases to around 700 for the $\tau = 25$ cases. The SNR reaches a minimum of 72 in an absorption band channel in a $\tau = 5$ case, and a maximum of 763 in a weakly absorbing channel in a $\tau = 25$ case.

Forty true cloud cases are used with five of each case where optical depth ranges from 5 to 40 in increments of 5 and cloud-top pressure is randomly selected to be between 680—900 hPa and rounded to the nearest 10 hPa. The prior cloud properties are assumed to be unbiased, so are randomly sampled from a Gaussian with a mean equal to the truth and a standard deviation equal to the prior errors above. Each synthetic retrieval begins with a separate prior, and the prior is also used as the first guess.”

11. P10, L7. Do these 75 channels have the same wavelenghts for all test cases?

→ **Response:** Yes, text added and we have added reminders and clarifications throughout. You're right that this is an important point!

→ **Changes made:** p5L6 text added: “but will select a consistent micro-window of the same channels for each.”

P10L13—p10L15 now reads: “While this may result in a different location for each size of micro-window, the location is fixed for an individual case, i.e. the 5-channel microwindow consists of the same 5 channels in all 216 cases.”

5

P12L18—p12L20 reads: “the 75 channel micro-window containing the OCO-2 channels 353—426 (indices counting from 1 for the full 1,016 OCO-2 L1bSc channels) consistently satisfies our P_{top} and ΔP_c criteria and reduces the full wavelength range from 759.2—771.8 nm to 763.5—764.6 nm.” [inclusion of channel indices helps imply it’s fixed]

10

New Figure 6 shows the selected channels.

12. P11, last sentence. what is proposed here is a strong statement. What is the basis to support that "assumptions made here don't affect primary conclusion" here?

15

- **Response:** Fair point
- **Changes made:** Text removed.

20

13. Finally, it is not all that clear if measurement in O2 A with such a finer spectral resolution will be needed? In other words, using 75 channels vs. using just one channel (such as from EPIC, MERES or TROPOMI) for cloud retrievals, are there huge differences? Answering this question will greatly improve the impact of this paper.

25

- **Response:** We now report the spectral resolution requirements given by O’Brien & Mitchell and Heidinger & Stephens. We also reproduced a calculation similar to Schuessler et al. and get the same answer: that GOME-2 spectral resolution isn’t enough to obtain the three pieces of information we require. Our expanded introduction now explains that two A-band channels are insufficient (implicitly addressing MERIS, though we use POLDER as an example). We also now discuss TROPOMI – it has the nominal spectral resolution, its larger spatial resolution will be a disadvantage in heterogeneous scenes however.

30

- **Changes made:** p2L29—p2L30 text added: “However, older theoretical work suggested that a spectral resolution of better than 1 cm⁻¹ (O’Brien and Mitchell, 1992) or even 0.5 cm⁻¹ (Heidinger and Stephens, 2000) is required for an effective A-band retrieval that includes cloud geometric thickness.”

35

New Figure 6 and p12L21—p12L28 text added: “Figure 6 shows an example cloudy scene spectrum simulated for OCO-2 and highlights the chosen 75 channel micro-window in red. Also shown is an approximated GOME-2 spectrum based on the MetOp-B instrument characteristics (Munro et al., 2016). We approximate the ILS using Gaussian instrument line shapes, taking the 0.21 nm spectral sampling from Table 1 and FWHM of 0.50 nm from Table 2 of Munro et al. (2016). While OCO-2 spectra allow 3 independent pieces of information to be obtained (see the reported d_s in the figure caption) our calculations agree with previous work that the GOME-2 resolution only provides approximately 2 (Schuessler et al., 2014). Consistent with older theoretical work (Heidinger and Stephens, 2000; O’Brien and Mitchell, 1992) this analysis supports the case that OCO-2’s high spectral resolution leads to additional information about cloud geometric thickness.”

40

45

Information content of OCO-2 oxygen A-band channels for retrieving marine liquid cloud properties

Mark Richardson¹, Graeme L. Stephens^{1,2}

¹Jet Propulsion Laboratory, California Institute of Technology, Pasadena, CA 91125, U.S.A.

5 ²Department of Meteorology, University of Reading, Reading, RG6 6BB, U.K.

Correspondence to: Mark Richardson (markr@jpl.nasa.gov)

Abstract. An information content analysis is used to select channels for a marine liquid cloud retrieval using the high-spectral-resolution oxygen A-band instrument on NASA’s Orbiting Carbon Observatory-2 (OCO-2). Desired retrieval properties are cloud optical depth, ~~cloud pressure thickness and~~ cloud-top pressure and cloud-pressure thickness, which is the geometric thickness expressed in hPa, and the optimal channels depend on the atmospheric state, cloud properties and position within the OCO-2 swath. Based on information content criteria we select a micro-window of 75 of the 853 functioning OCO-2 channels spanning 763.5—764.6 nm and perform a series of synthetic retrievals with perturbed initial conditions. We estimate posterior errors from the sample standard deviations and obtain ± 0.75 in optical depth, ± 12.9 hPa in both cloud-top pressure and cloud pressure thickness, although removing the 10 % of samples with the highest χ^2 reduces posterior error in cloud-top pressure to ± 2.9 hPa and cloud pressure thickness to ± 2.5 hPa. The application of this retrieval to real OCO-2 measurements is briefly discussed, along with limitations and the greatest caution is urged regarding the assumption of a single homogeneous cloud layer, which is often, but not always, a reasonable approximation for marine boundary layer clouds.

1 Introduction

The oxygen A-band spans wavelengths with a wide range of absorption strength ~~and with sufficient spectral resolution these absorption differences which~~ can be exploited to determine photon path lengths and therefore retrieve ~~the altitude of~~ cloud top heights and potentially the within-cloud photon path, which is related to droplet number concentration and therefore cloud thickness. Meanwhile, ~~continuum reflectance allows a retrieval of~~ cloud optical depth can be retrieved from reflectance in approximately non-absorbing “continuum” channels (Fischer and Grassl, 1991a; Koelemeijer et al., 2001; Stephens and Heidinger, 2000). Such a retrieval that includes cloud geometric thickness or droplet number density would allow evaluation of model cloud physics (Bennartz, 2007) ~~and i.~~ In addition A-band retrievals use reflected sunlight so are physically independent from other common sources of cloud information such as longer wavelength infrared, which may mis-identify cloud-top pressure in the presence of temperature inversions (Baum et al., 2012).

The photon path length of reflected sunlight is estimated by comparing radiance between channels with different absorption characteristics. With known absorption coefficients and similar scattering and reflection properties between the channels, the photon path length is easily determined from the Beer-Lambert Law. This technique was first suggested as a way of

determining cloud-top altitude using the strong carbon dioxide (CO_2) absorption band near $2.0 \mu\text{m}$ with an atmospheric window near $2.1 \mu\text{m}$ (Hanel, 1961). ~~Soon after~~ Subsequently the oxygen A-band near $0.76 \mu\text{m}$ was proposed as it offers improved signal to noise (SNR) and avoids overlap with the $1.87 \mu\text{m}$ water vapour absorption band (Yamamoto and Wark, 1961). It was noted that clouds are not “simple diffuse reflectors” and that “absorption along the scattering paths within the clouds must be considered”.

With a single measured ratio of two channels it is only possible to determine the total photon path length and not distinguish between above-cloud and within-cloud components, as this would mean obtaining two pieces of information from a single measurement. One way of distinguishing is to take multiple measurements from diverse viewing angles, as is done by the Polarization and Directionality of the Earth’s Reflectances (POLDER) instrument series (Deschamps et al., 1994). POLDER-3 has a “narrow” channel with a full-width at half maximum (FWHM) of 10 nm centred at $\lambda = 763\text{nm}$, and a “wide” channel of FWHM 40 nm centred at 765 nm. Statistics of the inferred photon path from different angles have been shown to be related to the cloud centroid pressure (Ferlay et al., 2010), results of which have been tested against CloudSat radar and Cloud-Aerosol Lidar and Infrared Pathfinder Satellite Observations (CALIPSO) data (Desmons et al., 2013). A more recent study used an information content analysis based around the characteristics of the Multiviewing, Multi-channel and Multi-polarization Imaging (3MI) and the Multiangle SpectroPolarimetric Imager (MSPI) instruments. This concluded that multiangle measurements are informative about cloud geometric thickness, particularly for clouds thicker than 2—3 km (Merlin et al., 2016), which notably excludes the marine stratocumulus regime.

Another proposal to obtain additional measurements that inform about cloud geometric thickness is to combine paired measurements from both the oxygen A-band and B-band, as is such as those available from the Earth Polychromatic Imaging Camera (EPIC) on the Deep Space Climate Observatory (DSCOVR). By considering the sum and differences of the channel ratios it has been proposed that cloud geometrical thickness can be retrieved when cloud optical depth (τ) is greater than 5 (Yang et al., 2013).

An alternative to multiple angles or additional bands is to measure more channels in the A-band, as was done for the Scanning Imaging Absorption SpectroMeter for Atmospheric Chartography (SCIAMACHY) on board ENVISAT (Rozanov and Kokhanovsky, 2004), which when combined with the Global Ozone Monitoring Experiment instruments (GOME and GOME-2), provide a continuous A-band record since 1995. An information content analysis based on GOME-2 characteristics, using a spectral resolution of 0.2 nm and assumed signal-to-noise (SNR) of 100 showed that 2 pieces of information could be obtained (Schuessler et al., 2014). This study showed the best performance when retrieving cloud-top height with either τ or cloud fraction and reported that there was not sufficient information in these assumed measurements to obtain cloud geometric thickness with “satisfactory accuracy”.

However, older theoretical work suggested that a spectral resolution of better than 1 cm^{-1} (O’Brien and Mitchell, 1992) or even 0.5 cm^{-1} (Heidinger and Stephens, 2000) is required for an effective A-band retrieval that includes cloud geometric thickness. In wavelength terms this is 0.03—0.06 nm, and is now achieved by instruments carried by the Chinese Feng-Yun 3 series (most recently FY-3D), the Japanese Greenhouse Gas Observing Satellite (GOSAT), the European Sentinel-5 Precursor

(Sentinel-5P, which carries the Troposphere Measuring Instrument “TROPOMI”) and NASA’s Orbiting Carbon Observatory-2 (OCO-2).

This study considers OCO-2 and extends previous work that developed a lookup table to retrieve cloud-top pressure and optical depth for single layer liquid clouds over ocean (Richardson et al., 2017).

5 The Orbiting Carbon Observatory 2 (OCO-2) has high spectral resolution so was selected by (Richardson et al., 2017) for a simple cloud property retrieval with a model derived lookup table. This ~~table~~ simple retrieval combined 20 of OCO-2’s 853 functioning A-band channels into 2 “super-pixels” or “super-channels” based on their O₂ absorption. The lookup tables were used for all locations and weather conditions and were validated using collocated Moderate-resolution Imaging Spectroradiometer (MODIS) and CALIPSO data (Taylor et al., 2016). Here we develop an optimal-estimation-based retrieval (Rodgers, 2000) for single-layer water clouds over oceans using nadir-view OCO-2 measurements and subject it to several idealised tests. This study’s new contributions are goes beyond (Richardson et al., 2017) by (i) considering information content aspects to select groups of channels rather than combined super-channels, (ii) accounting for local meteorological conditions and (iii) adding cloud pressure thickness to the retrieved state. We express cloud geometric thickness in terms of hPa and refer to it as cloud pressure thickness, using with the symbol ΔP_c vector. Our current analysis considers aerosol-free cases as aerosols have not yet been properly implemented in our modified cloudy-sky version of the radiative transfer model, this is an avenue for future work and will be discussed in Sect. 5.

OCO-2 has 1,016 A-band channels of which 853 function across all soundings and channels are separated in wavelength by just with spectral sampling between over 0.01–0.02 nm with a and a FWHM of 0.04 nm in wavelength, implying sufficient spectral resolution for geometric thickness retrievals. Low marine clouds are the primary cause of spread in net modelled cloud feedback (Bony and Dufresne, 2005; Zelinka et al., 2012) and we focus on these clouds, which complements the multi-angular retrievals from other sensors which appear to perform better for thicker clouds (Ferlay et al., 2010; Merlin et al., 2016). OCO-2 is also promising as its SNR values commonly range from 300–800 in cloudy scenes and it flies in the A-train constellation (L’Ecuyer and Jiang, 2010), allowing collocation with other sensors. Furthermore, its footprint size of approximately typically ranges from 1.2–2.3 km ~~1.4×2.2 km²~~ at nadir and compares favourably with both GOSAT (10.5 km diameter) and Sentinel-5P TROPOMI (7×7 km²), although its narrow swath of approximately 10 km is much reduced compared with TROPOMI’s 2600 km.

Here we aim to develop a computationally efficient cloud retrieval for OCO-2 by and here we selecting channels that contain the most information about the retrieved state properties, which speeds both the radiative transfer simulation and the optimal estimation calculations. In principle, the particular set of optimal channels may depends on the exact cloud case and on the across-track position of the measurement because the instrument line shapes (ILS) vary across the swath. Furthermore, neighbouring ILS overlap so it is more computationally efficient to select neighbouring pixels channels since the radiative transfer will already have been calculated for many of the relevant frequencies. We refer to the selection of neighbouring channels as a “micro-window” approach and use the OCO-2 Level 2 Full Physics Radiative Transfer Model (L2FP RTM,

(Boesch et al., 2015)) with a set of representative atmosphere and liquid cloud states to select the optimal micro window based on information content and posterior error criteria.

~~In principle, obtaining the three properties τ , P_{top} and ΔP_e might require only three independent channels. However, the optimal set would require knowing the cloud state beforehand, so we aim to select the smallest set of neighbouring channels that will allow accurate retrievals across the full range of cloud cases.~~

~~This approach aims to optimise a cloud property retrieval and due to limitations related to the radiative transfer implementation and computational burden, droplet size is not a retrieved property, instead it but contributes to the posterior uncertainty. It has been suggested that above-cloud CO_2 retrievals have been found to require cloud ~~can be retrieved if cloud properties are well known, including the effective droplet radius size for good accuracy~~ (Vidot et al., 2009) and therefore our current implementation will not directly lead to above-cloud CO_2 retrievals.~~

The paper is organised as follows: Sect. 2 describes the OCO-2 satellite measurements, radiative transfer model and general information content approach. Sect. 3 details the methodology specific to this paper, including the sample atmospheres, perturbations for determining covariance matrix components, the sequential channel selection procedure and information content and retrieval analysis. Sect. 4 reports the results of each of these cases, Sect. 5 discusses the results and describes how they will be applied in the real OCO-2 cloud retrieval, and Sect. 6 concludes.

2 ~~Data sources and analysis techniques~~The OCO-2 satellite and its instruments

The OCO-2 satellite orbits in a Sun-synchronous orbit as part of the A-train constellation (L'Ecuyer and Jiang, 2010). It follows a 16-day repeat cycle ~~with an at the e~~Equator ~~with a~~ crossing time near 13:30 in the ascending node and follows the CloudSat and CALIPSO reference ground track. OCO-2 has three viewing modes: a target mode for in-flight validation plus glint and nadir modes for operational measurements. Currently the satellite alternates nadir and glint orbits with some ocean orbits dedicated entirely to glint mode. Here we use nadir soundings to allow future cross-comparisons with the nadir-view instruments on CloudSat and CALIPSO. Several nadir orbits pass over marine stratocumulus regions ~~where where these measurements~~OCO-2 offers unique value in terms of determining cloud geometric thickness, for clouds that are thick enough to attenuate ~~and multiply scatter~~ the CALIPSO lidar (Vaughan et al., 2009), and low enough that CloudSat suffers significantly from surface clutter (Huang et al., 2012). ~~as CloudSat measurements are further well as being~~ limited in terms of vertical resolution by the radar bin size which is downsampled to 240 m (Stephens et al., 2008). Currently, the main OCO-2 products are for column atmospheric CO_2 ~~abundance concentration~~ (XCO₂ (Crisp, 2008; Crisp et al., 2016; Eldering et al., 2016; Osterman et al., 2016)) and solar-induced fluorescence (SIF, (Frankenberg et al., 2014)) which only use clear-sky soundings. ~~Since any footprint that is identified as possibly cloudy is not processed in the standard OCO-2 products. This work therefore~~ generates value from largely unused soundings.

OCO-2 functions in a pushbroom fashion with the footprint size depending on the viewing mode, but typically being 1.2—2.3 km. There are 8 across-track soundings, and each set of these is referred to as a frame in OCO-2 nomenclature. Within each

sounding, measurements of reflected sunlight are taken in the oxygen A-band, weak-CO₂ and strong-CO₂ bands. The CO₂ bands are not considered in this analysis but do contain information about cloud phase and droplet or particle size (Nakajima and King, 1990), and this information is-will be used when this retrieval is applied in our observation-based study to identify likely liquid cloud cases.

5 The OCO-2 A-band instrument is a bore-sighted, imaging, grating spectrometer that measures 1,016 channels spanning the wavelengths 759.2—771.8 nm. It is a flight spare from the original OCO mission and a number of pixels-focal plane array (FPA) elements have failed. 853 of the 1,016 channels are available across all soundings and over 94 % of the damaged pixels channels occur in the A-band continuum where there is redundancy, meaning little loss of information (Richardson et al., 2017).

10 This redundancy extends to the remaining undamaged pixelsFPA elements, meaning that fewer channels may be used to reduce the computational burden of a retrieval. The minimum number of channels required is equal to the number of elements in the retrieval state vector, provided that the channel responses to changes in the state vector properties contain orthogonal components. Therefore, for our desired retrievals of optical depth, physical thickness and cloud-top pressure, a single cloud retrieval requires at least 3 channels. The purpose of this study is to determine how many channels are required to cover a
15 range of realistic cloud cases and to identify those channels.

A quirk of the OCO-2 instrument complicates this determination. The wavelength of channels varies slightly between across-track soundings, which means that the sampled oxygen absorption coefficient also varies. For this reason we separately analyse each of the 8 frame sounding positions but will select a consistent micro-window of the same channels for each.

2.1 OCO-2 radiative transfer calculations

20 We use the OCO-2 Level 2 Full Physics Radiative Transfer Model (L2RTM) that was developed for the OCO-2 XCO₂ retrieval. Associated wrapper code handles inputs such as interpolated ECMWF meteorological fields and accounts for the OCO-2 satellite orbit, viewing geometry and instrumental response as described in the OCO-2 data version 6 documentation (Boesch et al., 2015). The radiative transfer is based on the VLIDORT radiative transfer model with a correction for the first two orders of scattering (Natraj and Spurr, 2007; Spurr, 2006; Spurr et al., 2001) that fundamentally follows the eigenvector
25 approach to solving the radiative transfer equation (Flatau and Stephens, 1988). This model accounts for Earth's curvature for calculating atmospheric path length of the incident and reflected solar beam, but is otherwise horizontally homogeneous. More details are provided in (Spurr, 2006) and (O'Dell, 2010).

Although the L2RTM was designed for clear-sky XCO₂ retrievals, it has been validated in cloudy atmospheres by comparing OCO-2 observations with L2RTM output assuming collocated MODIS and CALIPSO cloud properties (Richardson et al.,
30 2017). For homogeneous single-layer liquid clouds over ocean, the root mean square error (RMSE) in continuum channels was ± 18 %, an overestimate of the model-only error as this includes 3d cloud effects, collocation error, parallax effects and uncertainty in the MODIS and CALIPSO retrievals.

Clouds are implemented as follows: the atmosphere is defined on 20 levels, of which one is defined as the cloud centre, one as the cloud top and one as the cloud bottom. The cloud top is placed at the cloud-top pressure and the other cloud levels are equidistantly spaced to cover the cloud-pressure thickness. An extinction coefficient is assigned to the centre level to result in the desired optical depth. Above the cloud the pressure levels are linearly interpolated from the cloud top to 1 Pa. Below the cloud they are linearly interpolated from the cloud bottom to the surface pressure. The level selected for the cloud centre is that whose pressure is closest to the cloud centre when linearly interpolated across the 20 levels from the surface pressure to 1 Pa. The L2RTM assigns extinction coefficients to layers by interpolating between levels, so a vertically homogeneous cloud layer is assumed.

Mie scattering computations are used within clouds using relevant coefficients that are pre-calculated for gamma distributions of cloud droplets based on a summary of low-cloud studies (Miles et al., 2000). These values have only been pre-computed for integer values of effective droplet size. This should not affect our results greatly since our calculated uncertainties include a term spanning a range of droplet sizes. Water surfaces at nadir are dark, and even in cloud-free cases there is rarely sufficient SNR for the OCO-2 algorithm to attempt an XCO₂ retrieval. We assume a Cox-Munk surface reflectance function with the L2RTM surface reflectance set to 0.10, but as we only use nadir view over ocean there is little sensitivity to surface properties.

2.2 Optimal estimation and information content

We follow the principles of optimal estimation from (Rodgers, 2000), where a Bayesian retrieval combines an observation vector \mathbf{y} with a prior state vector \mathbf{x}_a and obtains a posterior state $\hat{\mathbf{x}}$. In our case the state vector consists of cloud-top pressure P_{top} , cloud pressure thickness ΔP_c and cloud optical depth τ . This assumes that the observation can be related to the state by a linear forward model with some error ϵ :

$$\mathbf{y} = \mathbf{K}\mathbf{x} + \epsilon \quad (1)$$

Where we refer to \mathbf{K} as the Jacobian matrix as its elements are $K_{i,j} = \partial y_i / \partial x_j$. Assuming Gaussian distributions associated with \mathbf{x}_a and \mathbf{y} , (Rodgers, 2000) shows that the best estimate of the posterior state is:

$$\hat{\mathbf{x}} = \mathbf{x}_a + \mathbf{S}_a \mathbf{K}^T (\mathbf{K} \mathbf{S}_a \mathbf{K}^T + \mathbf{S}_\epsilon)^{-1} (\mathbf{y} - \mathbf{K} \mathbf{x}_a) \quad (2)$$

And its covariance matrix is:

$$\hat{\mathbf{S}} = (\mathbf{K}^T \mathbf{S}_\epsilon^{-1} \mathbf{K} + \mathbf{S}_a^{-1})^{-1} \quad (3)$$

Here \mathbf{S}_a is the prior covariance and \mathbf{S}_ϵ the observation covariance. From Eq. (2) the posterior state $\hat{\mathbf{x}}$ is the prior \mathbf{x}_a plus an iteration that is based on the difference between the observed and expected \mathbf{y} with appropriate weighting for uncertainties. Eq. (3) shows that the reduction in posterior uncertainty $\hat{\mathbf{S}}$ is reduced by an amount that depends on the size of the Jacobian \mathbf{K} weighted by the observation uncertainty \mathbf{S}_ϵ . Potential nonlinearity in $\mathbf{y}(\mathbf{x})$ is addressed by iteration, with the linear expansion being determined about each iteration step.

In our OCO-2 cloud retrieval the state vector contains optical depth, cloud pressure thickness and cloud-top pressure while the observation state-vector is any subset of the 853 valid OCO-2 A-band channels. Using fewer channels reduces the

computational burden, both in terms of the radiative transfer and for iterating the retrieval which would otherwise involve repeated inversion of 853×853 matrices.

It is common practice to select channels based on information content and/or degrees of freedom for signal (Chang et al., 2017; Mahfouf et al., 2015; Martinet et al., 2014; Rabier et al., 2002), and this approach has already been used in an oxygen A-band

5 and B-band analysis for aerosol retrievals (Ding et al., 2016).

The information content is based on the concept of Shannon entropy and is related to the volume of state space occupied by the probability distribution P that represents our knowledge:

$$S(P) = -\sum_i P(x_i) \log_2 P(x_i) \quad (4)$$

It is expressed in bits, which represents the number of binary digits required to represent the possible outcomes. A retrieval decreases the probability distribution volume, and this change in associated Shannon entropy (Shannon and Weaver, 1949) is the information content, IC , of the measurements:

$$IC = S(P_0) - S(P_1) \quad (5)$$

In this case $S(P_0)$ is the Shannon entropy associated with the original probability distribution and $S(P_1)$ the same value associated with the retrieved probability distribution. For multivariate Gaussian descriptions of the probability distributions,

15 (Rodgers, 2000) shows that the information content of measurements is:

$$IC = \frac{1}{2} \ln |S_a| - \frac{1}{2} \ln |\hat{S}| = \frac{1}{2} \ln |S_a \hat{S}^{-1}| \quad (6)$$

A related property is the degrees of freedom for signal, d_s , which represents the number of useful independent quantities in a measurement. It may be thought of as how many different variables can be obtained from a measurement and with our three-component state vector we require a value approaching three. It may be calculated from the prior and posterior state covariances as:

$$d_s = \text{tr}(\mathbf{1} + \hat{S} S_a^{-1}) \quad (7)$$

Note the different order and inversion state of the covariance matrices relative to Eq. (6). In our analysis we calculate ~~information content~~ IC , d_s , and posterior errors for continuous micro-windows of varying size and these calculations require S_e and S_a . We assume prior covariances based partially on ~~the a~~ MODIS and CALIPSO cross-validation ~~from~~ (Richardson et al., 2017), and calculate the observation covariance S_e by perturbing atmospheric profiles. The calculation of the covariances is described in Sect. 3.1 and the channel selection approach in Sect. 3.2.

While theoretically 3 channels is sufficient to retrieve 3 state vector elements, it is not clear that the same 3 channels will apply in all cases. For example, while changes in cloud-top pressure of higher clouds may lead to strong responses in channels near line cores, light in these channels may be mostly absorbed by the time it reaches lower clouds, so less-strongly absorbing channels will be preferred for lower clouds. Changes in absorption due to temperature or water vapour may also affect the relative response of radiances to cloud properties. For this purpose, we consider a variety of atmospheric and cloud properties. Necessary observation covariances are derived by perturbing atmospheric profiles and the ~~IC information content~~ d_s and posterior covariance are used to select an optimal micro-window. Finally a retrieval is developed and tested on cloudy

atmospheres where the “truth” is assigned and pseudo-observations and prior values are provided by sampling from the previously defined covariance matrices.

3 Methodology, ~~and example atmospheric states and cloud states~~ cases

For ease of presentation we restrict our analysis to three representative atmospheric states, three cloud heights (680 hPa, 750 hPa and 850 hPa) and three cloud optical depths (5, 10 and 25). Together, this results in 27 combination cases. Effective droplet radius is assumed to be 12 μm , and cloud-pressure thickness is determined from the cloud geometric thickness from ~~the a~~ subadiabatic stratiform cloud model (Borg and Bennartz, 2007):

$$H = \sqrt{\frac{2LWP}{C_w}} \quad (8)$$

Where C_w is the moist adiabatic condensate coefficient and for marine stratocumulus we use $1.9 \times 10^{-3} \text{ g m}^{-4}$ (range given as 1— $2.5 \times 10^{-3} \text{ g m}^{-4}$ from (Brenguier, 1991)) and LWP is the liquid water path which is related to optical depth τ and effective droplet radius r_{eff} :

$$LWP = \frac{\tau r_{eff}^{10} \rho_w}{9 Q_{ext}} \quad (9)$$

Where ρ_w is the density of water and Q_{ext} the area-weighted mean scattering efficiency (Szczodrak et al., 2001), which we take to be 2. This value is chosen as it represents the large-particle limit for non-absorbing spheres (Herman, 1962) which is a reasonable approximation for cloud droplets in the oxygen A-band. A pressure scale height of 8 km is assumed to convert the resultant eCloud geometric thickness is converted to pressure thickness by assuming that pressure decreases exponentially with altitude with a scale height of 8 km. Note that the combined Eq. (8) and Eq. (9) is result comes from an adiabatic cloud model in which the LWP increases linearly with height, and differs by a factor of 5/6 from the classic result derived for a homogeneous cloud profile (Stephens, 1978). Neither assumption is perfectly representative of reality, but the adiabatic profile is expected to be more realistic so is used here.

For the representative atmospheric states, we select all collocated soundings that are identified as single-layer liquid clouds by both MODIS and CALIPSO during November 2015 and bin them according to absolute latitude, in the ranges 0—20°, 20—50° and 50—90°. The MODIS data are from product MYD06 at 1 km horizontal resolution (Platnick et al., 2015) and the CALIPSO data are from the 1 km resolution cloud layer product 01kmCLay (Vaughan et al., 2009). Within each bin Then the collocated OCO-2 ECMWF-AUX meteorological profiles (including pressure, specific humidity, temperature and wind speed) assigned to each of these soundings are taken and within each bin all of the profiles are averaged level-by-level. This includes all meteorological inputs used by the L2RTM, such as pressure, temperature, humidity and wind speed.

3.1 Calculation of observation covariances

For simplicity we assume that the components of \mathbf{S}_ϵ are independent and consider error contributions from instrumental uncertainty \mathbf{S}_I , and that introduced by uncertainty in the temperature profile \mathbf{S}_T , humidity profile \mathbf{S}_q and effective droplet radius $\mathbf{S}_{r_{eff}}$ such that:

$$5 \quad \mathbf{S}_\epsilon = \mathbf{S}_I + \mathbf{S}_T + \mathbf{S}_q + \mathbf{S}_{r_{eff}} \quad (10)$$

In reality, the temperature and humidity uncertainties are likely to be correlated, but this simplifies the calculation and allows unique attribution of covariance sources. The matrix \mathbf{S}_I is a diagonal matrix so averaging over more channels reduces the total posterior uncertainty even if the Jacobians are not independent. Its elements are equal to the square of the instrumental uncertainty, which depends on the radiance.

10 For \mathbf{S}_T and \mathbf{S}_q we follow the approach of (Chang et al., 2017) and perturb the tropical, mid-latitude and high-latitude atmospheric profiles 2,000 times for temperature or humidity separately ~~with~~ ~~U~~ ~~uncertainties~~ ~~are~~ ~~based~~ ~~on~~ ~~the~~ ~~1~~ ~~km~~ ~~resolution~~ AIRS validation results (Divakarla et al., 2006). For temperature we add a uniform perturbation to each level with a value sampled from a zero mean (μ) Gaussian with standard deviation (σ) of ± 1.5 K. For specific humidity we sample from a zero mean Gaussian with a standard deviation of unity, then scale this value based on pressure level. The scaling is equivalent to
15 ± 20 % of the initial specific humidity at the surface, increasing linearly to ± 50 % of the layer values at 250 hPa and remaining at ± 250 hPa% for levels with lower pressure. and are ± 1.5 K in temperature and for specific humidity, scale linearly from ± 20 % at the surface to ± 50 % at 250 hPa. At higher altitudes, ± 50 % is used at all levels. For each perturbed temperature simulation, the entire temperature profile is uniformly perturbed by a single value sampled from a zero mean Gaussian with standard deviation ± 1.5 K. For specific humidity, we sample from a zero mean Gaussian with unit standard deviation and multiply that
20 value by the percentage scaling profile described above. The calculation was also performed with 2,000 perturbations applied to r_{eff} assuming by sampling from a lognormal distribution that approximates the effective radius distribution reported by MODIS for our November 2015 low cloud cases. This lognormal fit has an arithmetic mean of $12.0 \mu\text{m}$, but after excluding values outside the $4\text{--}30 \mu\text{m}$ retrieved by MODIS, with a mean of $12.6 \mu\text{m}$ and $5\text{--}95$ % range of the values fall within $7.5\text{--}19.4 \mu\text{m}$ the arithmetic mean is $12.6 \mu\text{m}$ and $5\text{--}95$ % of the values fall within
25 $7.5\text{--}19.4 \mu\text{m}$. We choose $r_{eff} = 12 \mu\text{m}$ in our default retrieval as we are restricted to integer values by the available L2RTM Mie scattering tables, and based on its similarity to the full distribution mean.

For each set of perturbations, we simulated the A-band spectra for cloud optical depths of 5, 10 and 25 and solar zenith angles of approximately 30° , 45° and 60° with a cloud-top pressure of 850 hPa. We calculate covariances at a single value of P_{top} , but the convergence of our synthetic retrieval tests across a range of true P_{top} values shows that we obtain reliable results
30 regardless.

The output ~~was sampled with each of~~ spectra are provided for each of the 8 different instrument line shapes associated with the 8 different OCO-2 across-track sounding positions.

For each set of 2,000 perturbed outputs, we estimated the covariance matrix elements, $S_{i,j}$, where i, j refer to channel indices, as:

$$S_{i,j} = \sum_k (I_{i,k} - \langle I_i \rangle) (I_{j,k} - \langle I_j \rangle) / N \quad (11)$$

Where the sum is over the $N=2,000$ spectra of radiance I , which are individually referred to using the index k . In this case $\langle I_i \rangle$ and $\langle I_j \rangle$ are the sample mean radiances in the relevant pixels-channels i and j .

3.2 Channel selection

Eq. (3) and Eq. (6) state that we can determine the information content and posterior error covariance from the prior covariance, observation covariance and Jacobians. Our aim is to select the optimal micro-window of consecutive OCO-2 pixels-channels to provide a retrieval that efficiently reduces the posterior state error.

10 We use the L2FP radiative transfer model to simulate OCO-2 spectra for marine liquid clouds of τ in [5, 10, 25] and P_{top} in [680, 750, 850] hPa, for each of the 3 meteorological cases described in Sect. 3.1 and for each of the eight across-track sounding positions. In each case, the solar zenith angle is 45° and the Jacobians for τ, P_{top} and ΔP are determined by finite differencing. The relevant observation covariance is that determined for the same sounding position, region and optical depth in Sect. 2.2 at $SZA = 45^\circ$. Prior covariance is assumed to be diagonal, equivalent to an error of 1.5 in τ -error of ± 1.5 , of 60 hPa in P_{top} of ± 60
 15 hPa and of 7.5 hPa in ΔP of ± 7.5 hPa. Our τ prior error comes from applying the $\pm 15-18$ % error in simulated radiance for homogeneous clouds when provided with MODIS optical depth found in (Richardson et al., 2017). Our P_{top} uncertainty is approximately equal to that determined in the same study when comparing prior from the standard deviation of the differences between OCO-2 P_{top} with and CALIPSO P_{top} when using a simple lookup table for OCO-2, which we intend to use for the OCO-2 prior. The ΔP uncertainty is similar to the ± 20 % error associated with Eq. (87) for clouds of cloud fraction > 0.8
 20 reported in (Bennartz, 2007).

We consider the information content IC , and the 3 diagonal elements of the posterior covariance matrix \mathbf{S}_x . The information content accounts for non-diagonal terms in the posterior covariance, allowing an objective best selection, while the diagonal elements allow more intuitive interpretation of the magnitude of the posterior uncertainty. We refer to these using the symbol σ with a relevant subscript, such that $\sigma_\tau^2 = S_{\tau,\tau}$ where $S_{\tau,\tau}$ is the element of the covariance matrix corresponding to the $\tau - \tau$
 25 covariance. Note that we present the square-root of this value, i.e. σ .

This approach represents a sample of 27 unique cloud-meteorology cases across the 8 different sets of OCO-2 instrument line shapes, resulting in 216 total cases. When selecting the optimal micro-window for retrievals, it is necessary to select not just its location, but also its size (i.e. number of neighbouring pixels-channels within the micro-window).

To make this problem tractable, we select micro-windows of the following size: 5, 10, 25, 50, 75, 100, 150, 200 and: 500
 30 neighbouring channels. For each of these possible sizes we calculate IC_{d_s} and the diagonal posterior error terms for every overlapping micro-window of that size. For example, the 853 individual OCO-2 pixels-channels allow 849 overlapping 5-pixel channel micro-windows, for which we determine the information content values for each of the 216 cases.

For each size of micro-window we choose the one with the highest mean information content across the 216 cases. While this This may result in a different location for each size of micro-window, the location is fixed for an individual case, i.e. the 5-channel microwindow consists of the same 5 channels in all 216 cases, and we We select the optimal micro-window size as that with >80 % of the 500-channel IC, optical depth posterior $\sigma_{\tau,\tau}$ better than ± 0.05 and a posterior of better than ± 1 hPa in the pressure terms $\sigma_{P_{top},P_{top}}$ and $\sigma_{\Delta P,\Delta P}$ for all 216 cases. These thresholds are by nature subjective and arbitrary.

3.3 Theoretical retrieval test case

We perform synthetic retrievals with known true cloud cases in mid-latitude meteorology and a 45° solar zenith angle. For each cloud case we perform 50 retrievals using a 12 micron droplet size and the prior cloud state is sampled from Gaussian distributions with σ_τ of $\pm 30\%$, $\sigma_{P_{top}}$ of ± 60 hPa. Cloud pressure thickness is calculated from Eq. (87) with LWP from Eq. (89), and in the optimal estimation a prior $\sigma_{\Delta P}$ of $\pm 25\%$ is assumed. The atmospheric humidity and temperature profiles are perturbed by sampling from the same distributions used to derive the covariance matrices in Sect. 3.2 and the observed spectrum in each case is generated by taking the simulated spectrum from the “truth” case and perturbing it by sampling from the relevant covariance matrix that has been scaled for the cloud properties according to Sect. 3.2. The squared OCO-2 radiance uncertainties are added to the diagonal elements of the observation error covariance matrix with no cross correlation. We use the standard OCO-2 version 7 uncertainties, and SNR increases as the radiance in a given channel increases. The median SNR for an individual spectrum ranges from just over 400 for the $\tau = 5$ cases to around 700 for the $\tau = 25$ cases. The single-channel SNR reaches a minimum of 72 in an absorption band channel in a $\tau = 5$ case, and a maximum of 763 in a weakly absorbing channel in a $\tau = 25$ case.

Forty true cloud cases are used with five of each case where optical depth ranges from 5 to 40 in increments of 5 and cloud-top pressure is randomly selected to be between 680—900 hPa and rounded to the nearest 10 hPa. The prior cloud properties are assumed to be unbiased, so are randomly sampled from a Gaussian with a mean equal to the truth and a standard deviation equal to the prior errors above. Each synthetic retrieval begins with a separate prior, and the prior is also used as the first guess. The retrieval attempts assume $r_{eff} = 12 \mu\text{m}$ but the true r_{eff} is allowed to vary and is randomly sampled from a literature summary of marine stratocumulus results, scaled to ensure a mean value of $12 \mu\text{m}$ (Miles et al., 2000). The r_{eff} distribution effective variance is fixed in each case in order to use the pre-calculated scattering properties used with the L2RTM code, but given the wide range of effective mean values considered, it is not expected that allowing the effective variance to change would greatly affect the results.

For each of the 50 perturbed prior states and observation spectra, we perform a standard 10-iteration optimal estimation retrieval (Rodgers, 2000) using the Gauss-Newton solution to optimise each step. These retrievals are done using the 75 channel micro-window selected following Sect. 3.3. The sample means and standard deviations are then compared with the known true state and indicate the theoretical performance of the micro-window retrieval.

4 Results

Results are presented here for the first sounding position, which is left-most when facing northwards along track during the ascending node. Our conclusions are not affected by changing the sounding position. For illustration, we select the case of $SZA = 45^\circ$, $\tau = 10$ and $P_{top} = 850$ hPa then present the square root of the diagonal components of covariance matrices for temperature, humidity and effective radius in Figure 1. This shows both the absolute and fractional uncertainty in the radiance due to each factor. Droplet size dominates, consistently contributing near 3 % of the radiance, although the temperature uncertainty contributes up to 1.5 % in the darker absorption channels.

Figure 2 shows the full covariance matrices for each component using the same mid-latitude meteorology ~~and the same~~ cloud properties and SZA as Figure 1. The strongest and most consistent positive cross-correlations occur for the effective droplet size.

While the overall patterns are similar for different cloud optical depths, solar zenith angles or regional meteorology, the absolute values of the covariance matrices change. A retrieval requires an estimate of the error covariance that is relevant for the given measurement but these matrices are computationally intensive to prepare, and storing and accessing a large number of them would make the retrieval less efficient. We will therefore use a single set of retrieval matrices, one for each across-track sounding position, and then scale the matrix to account for changes in solar zenith angle, meteorology and optical depth.

Figure 3 shows the relationship between the observation covariance matrix excluding the instrumental term \mathbf{S}_I for $\tau = 10$, $SZA = 30^\circ$ and $\tau = 25$, $SZA = 60^\circ$ with mid-latitude meteorology. Only the upper-diagonal elements of each matrix have been plotted to avoid duplication and values are scaled by μ_0^{-2} , where $\mu_0 = \cos \theta_{SZA}$. There is a linear relationship between the two matrices meaning that one may be reconstructed from the other. The results are similar for tropical and high-latitude cases, and for all soundings.

4.2 Micro-window selection

Figure 4 shows ~~information content~~ I_C and d_s spectra using micro-windows consisting of 5, 75 or 200 OCO-2 ~~pixels~~ channels. Also shown are the posterior errors in cloud properties taken from the square roots of the diagonal components of \mathbf{S}_x .

In this cloud case (mid latitude, $\tau = 10$, $P_{top} = 850$ hPa), the greatest information content comes from selecting channels near absorption features and avoiding the far wings of the A-band where only optical depth is reliably retrieved, as these channels have little O_2 absorption and so are uninformative about photon path length. Otherwise, the 5-pixel-channel micro-window is most sensitive to its placement within the spectrum: information content varies from 4.4—9.4 bits depending on the micro-window's location.

Micro-windows that contain fewer ~~pixels~~ channels are more sensitive to changes in the instrument line shapes and cloud conditions. For example, for the 5-pixel-channel micro-window in Figure 4, the best-performing channel has an information content of 9.4 bits. However, for a different cloudy case: $\tau = 25$, $P_{top} = 680$ hPa, and for sounding position 8 instead of 1, the

information content is reduced to 6.0 bits. This is a substantial loss relative to the best possible micro-window for that cloud case, which has 8.4 bits of information.

To assess the relative trade-offs between increased speed and decreased performance we take the micro-window with the highest mean information content across all cases². We then plot the central value and full range of the 216 values for each selected micro-window size in Figure 5, along with our chosen thresholds as dashed lines in each panel. The median case in the 50 channel micro-window passes our IC threshold and in all cases passes the τ -uncertainty threshold, but it has multiple cases that fail the P_{top} and ΔP_c thresholds. By contrast, the 75 pixel-channel micro-window containing the OCO-2 pixels channels 353—426 (indices counting from 1 for the full 1,016 OCO-2 L1bSc pixelschannels) satisfies our criteria consistently satisfies our P_{top} and ΔP_c criteria and reduces the full wavelength range from 759.2—771.8 nm to 763.5—764.6 nm.

Figure 6 shows an example cloudy scene spectrum simulated for OCO-2 and highlights the chosen 75 channel micro-window in red. Also shown is an approximated GOME-2 spectrum based on the MetOp-B instrument characteristics (Munro et al., 2016). We approximate the ILS using Gaussian instrument line shapes, taking the 0.21 nm spectral sampling from Table 1 and FWHM of 0.50 nm from Table 2 of Munro et al. (2016). While OCO-2 spectra allow 3 independent pieces of information to be obtained (see the reported d_s in the figure caption) our calculations agree with previous work that the GOME-2 resolution only provides approximately 2 (Schuessler et al., 2014). Consistent with older theoretical work (Heidinger and Stephens, 2000; O'Brien and Mitchell, 1992) this analysis supports the case that OCO-2's high spectral resolution leads to additional information about cloud geometric thickness.

4.3 Theoretical retrieval case

Example synthetic retrieval iterations using the 75-channel micro-window are shown in Figure 7 for $\tau = 10$ and $\tau = 25$ cases, and convergence typically occurs within few iterations. Lines are coloured according to their χ^2 values and it is clear that this is larger for cases where the result settles away from the true state. The posterior sample standard deviations are presented in Table 1 for the full samples and for cases where we filter the results by excluding the 10 % of cases with the highest χ^2 in each case. The greatest effect of filtering by χ^2 is to reduce the uncertainty in the cloud-top pressure and cloud pressure thickness from 12.9 hPa to 2.9 hPa and 2.5 hPa respectively. The mean standard deviation in the τ retrieval is ± 0.75 across all cases, but this is inflated by a large value in the $\tau = 35$ cases.

5 Discussion

OCO-2 O₂ A-band spectra are rich in information about cloud properties. Continuum pixels-channels with little absorption respond strongly to cloud optical depth, while the radiance in absorption bands is dominated by photon path length, which increases with cloud-top pressure or cloud pressure thickness. The A channel's response to cloud properties depends largely on the its oxygen absorption coefficient in the given channel (Fischer and Grassl, 1991b; Koelemeijer et al., 2001; Stephens

and Heidinger, 2000), and ~~with-since~~ many ~~pixels-channels having-have~~ similar ~~oxygen~~ absorption coefficients; there is ~~much~~ redundant cloud information in OCO-2 spectra.

We ultimately selected 75 neighbouring channels as containing the majority of the cloud information. Observation covariance matrices were developed based on uncertainty related to the atmospheric temperature and humidity profiles, in cloud droplet effective radius and instrumental uncertainty. These covariances depend on the meteorological profile, solar zenith angle and cloud properties. ~~Additionally,~~ ~~and that as~~ instrument line shapes vary across the OCO-2 swath, ~~so~~ a separate covariance matrix is required for each of the eight across-track OCO-2 footprints. Fortunately, when cloud or meteorological properties change, the covariance matrix elements tend to be approximately linearly related ~~so, a~~ ~~allowing a~~ arbitrary covariance matrix ~~to-can~~ be reconstructed from ~~the covariance matrix for~~ a known case. There is greater spread in the reconstructed humidity component but this contributes a small fraction of the total covariance, which is dominated by uncertainty in the droplet radius, whose component is well reconstructed.

Using 75 channels substantially reduces the retrieval processing time relative to the 853 available channels, and its usefulness was demonstrated in a set of 8 synthetic test cases where a known cloud case was retrieved. In our perturbed tests the retrieval typically converged within 2 iterations, although a few cases converged on a local optimum instead of approaching the truth. Fortunately, these cases can generally be identified from the associated χ^2 , indicating that when this approach is applied to real OCO-2 data, it may be possible to flag cases where there is less confidence in the retrieval.

Our idealised posterior errors of ± 0.75 in optical depth and better than ± 3 hPa in cloud-top pressure and cloud pressure thickness are based on assuming that convergence can be identified from the χ^2 values, and that the cloud is single-layered and horizontally homogeneous within the OCO-2 field of view of approximately 1.4×2.2 km. This is a reasonable approximation in marine stratocumulus decks, where the typical length scale of variability in Liquid Water Path can be 10–30 km (Wood and Hartmann, 2006), but will be violated in many low level cloud cases such as at the edges of the stratocumulus-trade cumulus transition.

In addition, ~~the assumption of a single scattering layer is commonly broken~~: multi-layered clouds are ubiquitous (Li et al., 2015), although for overlying cirrus it may be possible to identify and flag many of these cases based on the inferred distribution of photon path lengths from A-band measurements (Min et al., 2004). ~~Alternatively,~~ ~~since~~ OCO-2 flies in the A-train, it would also be possible to use ~~information from~~ other sensors such as CALIPSO (which is now ~~de-orbiting/leaving the A-train~~) or MODIS to identify multi-layer cloud cases, or scenes in which there is heavy aerosol loading.

~~Cases of heavy aerosol loading are most common over the Namibian stratocumulus region with common occurrence in June-July-August (JJA) and a peak in September-October-November (SON). A combination of CALIPSO, CloudSat and International Satellite Cloud Climatology Project (ISCCP) data imply that in the SON Namibian stratocumulus region, approximately one-third of low clouds have overlying aerosol, and approximately half of these cases are smoke (Devasthale and Thomas, 2011; Winker et al., 2010). Scattering layers overlying a marine cloud tend to reduce in the effective retrieved cloud layer pressure due to the reduced mean path length of those photons reflected from the overlying layer (Vanbauce et al., 1998). Assessment of aerosol effects will be necessary in future work.~~

It was also assumed that the clouds will be reliably identified as liquid, and that a constant effective droplet size may be assumed. Droplet size variance has been included in terms of the observation covariance, but this limits our retrieved posterior covariance. Cloud identification is relatively simple for nadir A-band reflectance measurements over ocean, as for most solar zenith angles the surface is dark and cloudy scenes may simply be identified when reflectance exceeds some threshold. The

5 OCO-2 instrument also carries weak- and strong-CO₂ band spectrometers, and with ice absorbing more strongly than water in the near infrared we will be able to use well-known retrieval principles to obtain cloud phase (Nakajima and King, 1990).

Our assumptions mean that the true error of an OCO-2 based cloud retrieval will be larger than that reported here, but our results suggest that the use of a 75-channel micro-window is justified as the basis of an OCO-2 cloud retrieval for marine liquid cloud properties.

10 **6 Conclusions**

The OCO-2 satellite carries an O₂ A-band spectroradiometer with high spectral sampling ~~in terms of oxygen absorption coefficient~~. Our analysis supports that this spectral sampling is sufficient to, in principle, allow determination of the optical depth, cloud-top pressure and geometric pressure thickness of clouds. It has been demonstrated that observed OCO-2 spectra respond largely as expected to changes in cloud optical depth and cloud-top pressure (Richardson et al., 2017), but that study

15 did not use modern Bayesian techniques. Such techniques account for relevant conditions such as line broadening due to local meteorology and they also account for prior information and cross-correlation between the responses of individual channels.

Here we report that the OCO-2 A-band spectra contain much redundant information as a number of channels experience similar oxygen absorption. After accounting for observational errors associated with uncertainty introduced by meteorology, cloud droplet size and instrumental error, it was found that with a micro-window of 75 continuous channels, most of the information

20 from the full 853-channel spectrum is retained. In a perfectly linear theoretical case, posterior error in cloud-top pressure and cloud pressure thickness were reduced below ± 1 hPa and optical depth below ± 0.05 .

Using perturbed synthetic tests, the majority of cases approached the known truth and the full sample posterior errors averaged ± 0.75 in optical depth, ± 12.9 hPa in P_{top} and cloud pressure thickness. Cases that converged to a state away from the truth could generally be identified by their large χ^2 values, and removing the 10 % of worst cases reduced the posterior sample

25 standard deviation in P_{top} and ΔP_c was reduced to ± 2.9 and ± 2.5 hPa.

These results apply in an ideal theoretical case of a uniform single layer liquid droplet cloud, and retrieval errors will be larger in reality where these assumptions do not apply. However, violations of these assumptions such as real-world cloud heterogeneity, will likely have a similar effect on both the full spectrum and on our selected 75-channel micro-window. We therefore propose that these assumptions do not affect our primary conclusion regarding the relative performance of our

30 optimised retrieval versus a more intensive, full spectrum retrieval.

Acknowledgments This research described in this paper was performed at the Jet Propulsion Laboratory, California Institute of Technology sponsored by NASA. MR has been funded by the OCO-2 and CloudSat projects. MR would like to thank James McDuffie and Jussi Leinonen for providing radiative transfer and optimal estimation code assistance, plus Matt Lebsock, Annmarie Eldering, Mike Gunson, Chris O'Dell, Tommy Taylor, Heather Cronk and Aronne Merrelli for helpful technical discussions. The OCO-2 science data are available online from the NASA Goddard GES DISC at https://disc.gsfc.nasa.gov/datacollection/OCO2_L1B_Science_7.html.

References

- Baum, B. A., Menzel, W. P., Frey, R. A., Tobin, D. C., Holz, R. E., Ackerman, S. A., Heidinger, A. K. and Yang, P.: MODIS Cloud-Top Property Refinements for Collection 6, *J. Appl. Meteorol. Climatol.*, 51(6), 1145–1163, doi:10.1175/JAMC-D-11-0203.1, 2012.
- Bennartz, R.: Global assessment of marine boundary layer cloud droplet number concentration from satellite, *J. Geophys. Res.*, 112(D2), D02201, doi:10.1029/2006JD007547, 2007.
- Boesch, H., Brown, L., Castano, R., Christi, M., Connor, B., Crisp, D., Eldering, A., Fisher, B., Frankenberg, C., Gunson, M., Granat, R., McDuffie, J., Miller, C., Natraj, V., O'Brien, D., O'Dell, C., Osterman, G., Oyafuso, F., Payne, V., Polonsky, I., Smyth, M., Spurr, R., Thompson, D. and Toon, G.: Orbiting Carbon Observatory (OCO)-2 Level 2 Full Physics Algorithm Theoretical Basis Document, Pasadena, CA. [online] Available from: https://disc.gsfc.nasa.gov/OCO-2/documentation/oco-2-v6/OCO2_L2_ATBD.V6.pdf, 2015.
- Bony, S. and Dufresne, J.-L.: Marine boundary layer clouds at the heart of tropical cloud feedback uncertainties in climate models, *Geophys. Res. Lett.*, 32(20), L20806, doi:10.1029/2005GL023851, 2005.
- Borg, L. A. and Bennartz, R.: Vertical structure of stratiform marine boundary layer clouds and its impact on cloud albedo, *Geophys. Res. Lett.*, 34(5), doi:10.1029/2006GL028713, 2007.
- Brenguier, J.: Parameterization of the Condensation Process: A Theoretical Approach, *J. Atmos. Sci.*, 48(2), 264–282, doi:10.1175/1520-0469(1991)048<0264:POTCPA>2.0.CO;2, 1991.
- Chang, K.-W., L'Ecuyer, T. S., Kahn, B. H. and Natraj, V.: Information content of visible and midinfrared radiances for retrieving tropical ice cloud properties, *J. Geophys. Res. Atmos.*, 122(9), 4944–4966, doi:10.1002/2016JD026357, 2017.
- Crisp, D.: NASA Orbiting Carbon Observatory: measuring the column averaged carbon dioxide mole fraction from space, *J. Appl. Remote Sens.*, 2(1), 23508, doi:10.1117/1.2898457, 2008.
- Crisp, D., Pollock, H. R., Rosenberg, R., Chapsky, L., Lee, R. A. M., Oyafuso, F. A., Frankenberg, C., O'Dell, C. W., Bruegge, C. J., Doran, G. B., Eldering, A., Fisher, B. M., Fu, D., Gunson, M. R., Mandrake, L., Osterman, G. B., Schwandner, F. M., Sun, K., Taylor, T. E., Wennberg, P. O. and Wunch, D.: The On-Orbit Performance of the Orbiting Carbon Observatory-2 (OCO-2) Instrument and its Radiometrically Calibrated Products, *Atmos. Meas. Tech. Discuss.*, 1–45, doi:10.5194/amt-2016-

281, 2016.

Deschamps, P.-Y., Breon, F.-M., Leroy, M., Podaire, A., Bricaud, A., Buriez, J.-C. and Seze, G.: The POLDER mission: instrument characteristics and scientific objectives, *IEEE Trans. Geosci. Remote Sens.*, 32(3), 598–615, doi:10.1109/36.297978, 1994.

Desmons, M., Ferlay, N., Parol, F., Mcharek, L. and Vanbauce, C.: Improved information about the vertical location and extent of monolayer clouds from POLDER3 measurements in the oxygen A-band, *Atmos. Meas. Tech.*, 6(8), 2221–2238, doi:10.5194/amt-6-2221-2013, 2013.

Devasthale, A. and Thomas, M. A.: A global survey of aerosol-liquid water cloud overlap based on four years of CALIPSO-CALIOP data, *Atmos. Chem. Phys.*, 11(3), 1143–1154, doi:10.5194/acp-11-1143-2011, 2011.

Ding, S., Wang, J. and Xu, X.: Polarimetric remote sensing in O2 A and B bands: Sensitivity study and information content analysis for vertical profile of aerosols, *Atmos. Meas. Tech. Discuss.*, 1–47, doi:10.5194/amt-2015-340, 2016.

Divakarla, M. G., Barnet, C. D., Goldberg, M. D., McMillin, L. M., Maddy, E., Wolf, W., Zhou, L. and Liu, X.: Validation of Atmospheric Infrared Sounder temperature and water vapor retrievals with matched radiosonde measurements and forecasts, *J. Geophys. Res.*, 111(D9), D09S15, doi:10.1029/2005JD006116, 2006.

Eldering, A., O'Dell, C. W., Wennberg, P. O., Crisp, D., Gunson, M. R., Viatte, C., Avis, C., Braverman, A., Castano, R., Chang, A., Chapsky, L., Cheng, C., Connor, B., Dang, L., Doran, G., Fisher, B., Frankenberg, C., Fu, D., Granat, R., Hobbs, J., Lee, R. A. M., Mandrake, L., McDuffie, J., Miller, C. E., Myers, V., Natraj, V., O'Brien, D., Osterman, G. B., Oyafuso, F., Payne, V. H., Pollock, H. R., Polonsky, I., Roehl, C. M., Rosenberg, R., Schwandner, F., Smyth, M., Tang, V., Taylor, T. E., To, C., Wunch, D. and Yoshimizu, J.: The Orbiting Carbon Observatory-2: First 18 months of Science Data Products, *Atmos. Meas. Tech. Discuss.*, 1–30, doi:10.5194/amt-2016-247, 2016.

Ferlay, N., Thieuleux, F., Cornet, C., Davis, A. B., Dubuisson, P., Ducos, F., Parol, F., Riédi, J. and Vanbauce, C.: Toward New Inferences about Cloud Structures from Multidirectional Measurements in the Oxygen A Band: Middle-of-Cloud Pressure and Cloud Geometrical Thickness from POLDER-3/ PARASOL, *J. Appl. Meteorol. Climatol.*, 49(12), 2492–2507, doi:10.1175/2010JAMC2550.1, 2010.

Fischer, J. and Grassl, H.: Detection of Cloud-Top Height from Backscattered Radiances within the Oxygen A Band. Part 1: Theoretical Study, *J. Appl. Meteorol.*, 30(9), 1245–1259, doi:10.1175/1520-0450(1991)030<1245:DOCTHF>2.0.CO;2, 1991a.

Fischer, J. and Grassl, H.: Detection of Cloud-Top Height from Backscattered Radiances within the Oxygen A Band. Part 1: Theoretical Study, *J. Appl. Meteorol.*, 30(9), 1245–1259, doi:10.1175/1520-0450(1991)030<1245:DOCTHF>2.0.CO;2, 1991b.

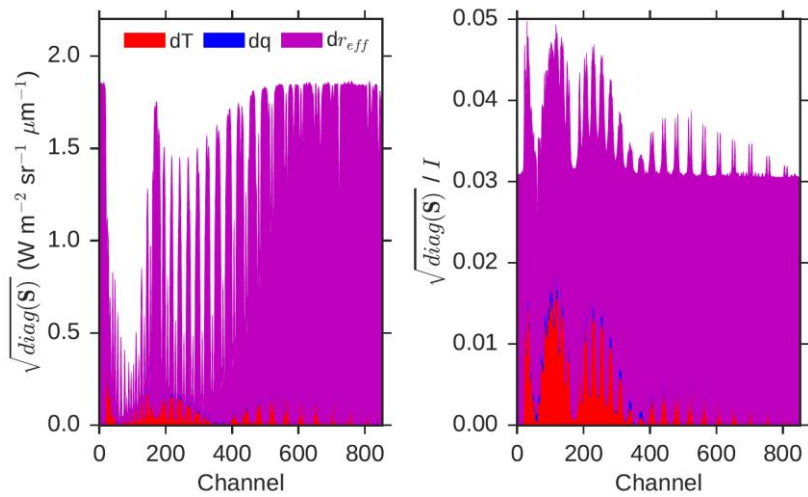
Flatau, P. J. and Stephens, G. L.: On the fundamental solution of the radiative transfer equation, *J. Geophys. Res.*, 93(D9), 11037, doi:10.1029/JD093iD09p11037, 1988.

Frankenberg, C., O'Dell, C., Berry, J., Guanter, L., Joiner, J., Köhler, P., Pollock, R. and Taylor, T. E.: Prospects for chlorophyll fluorescence remote sensing from the Orbiting Carbon Observatory-2, *Remote Sens. Environ.*, 147, 1–12, doi:10.1016/j.rse.2014.02.007, 2014.

- Hanel, R. A.: Determination of cloud altitude from a satellite, *J. Geophys. Res.*, 66(4), 1300–1300, doi:10.1029/JZ066i004p01300, 1961.
- Heidinger, A. K. and Stephens, G. L.: Molecular Line Absorption in a Scattering Atmosphere. Part II: Application to Remote Sensing in the O₂ A band, *J. Atmos. Sci.*, 57(10), 1615–1634, doi:10.1175/1520-0469(2000)057<1615:MLAIAS>2.0.CO;2, 5 2000.
- Herman, B. M.: Infra-red absorption, scattering, and total attenuation cross-sections for water spheres, *Q. J. R. Meteorol. Soc.*, 88(376), 143–150, doi:10.1002/qj.49708837604, 1962.
- Huang, Y., Siems, S. T., Manton, M. J., Hande, L. B. and Haynes, J. M.: The Structure of Low-Altitude Clouds over the Southern Ocean as Seen by CloudSat, *J. Clim.*, 25(7), 2535–2546, doi:10.1175/JCLI-D-11-00131.1, 2012.
- 10 Koelemeijer, R. B. A., Stammes, P., Hovenier, J. W. and de Haan, J. F.: A fast method for retrieval of cloud parameters using oxygen A band measurements from the Global Ozone Monitoring Experiment, *J. Geophys. Res. Atmos.*, 106(D4), 3475–3490, doi:10.1029/2000JD900657, 2001.
- L’Ecuyer, T. S. and Jiang, J. H.: Touring the atmosphere aboard the A-Train, *Phys. Today*, 63(7), 36–41, doi:10.1063/1.3463626, 2010.
- 15 Li, J., Huang, J., Stammes, K., Wang, T., Lv, Q. and Jin, H.: A global survey of cloud overlap based on CALIPSO and CloudSat measurements, *Atmos. Chem. Phys.*, 15(1), 519–536, doi:10.5194/acp-15-519-2015, 2015.
- Mahfouf, J.-F., Birman, C., Aires, F., Prigent, C., Orlandi, E. and Milz, M.: Information content on temperature and water vapour from a hyper-spectral microwave sensor, *Q. J. R. Meteorol. Soc.*, 141(693), 3268–3284, doi:10.1002/qj.2608, 2015.
- Martinet, P., Lavanant, L., Fourri?, N., Rabier, F. and Gambacorta, A.: Evaluation of a revised IASI channel selection for cloudy 20 retrievals with a focus on the Mediterranean basin, *Q. J. R. Meteorol. Soc.*, 140(682), 1563–1577, doi:10.1002/qj.2239, 2014.
- Merlin, G., Riedi, J., Labonnote, L. C., Cornet, C., Davis, A. B., Dubuisson, P., Desmons, M., Ferlay, N. and Parol, F.: Cloud information content analysis of multi-angular measurements in the oxygen A-band: application to 3MI and MSPI, *Atmos. Meas. Tech.*, 9(10), 4977–4995, doi:10.5194/amt-9-4977-2016, 2016.
- Miles, N. L., Verlinde, J. and Clothiaux, E. E.: Cloud Droplet Size Distributions in Low-Level Stratiform Clouds, *J. Atmos. Sci.*, 25 57(2), 295–311, doi:10.1175/1520-0469(2000)057<0295:CSDIL>2.0.CO;2, 2000.
- Min, Q.-L., Harrison, L. C., Kiedron, P., Berndt, J. and Joseph, E.: A high-resolution oxygen A-band and water vapor band spectrometer, *J. Geophys. Res.*, 109(D2), D02202, doi:10.1029/2003JD003540, 2004.
- Munro, R., Lang, R., Klaes, D., Poli, G., Retscher, C., Lindstrot, R., Huckle, R., Lacan, A., Grzegorski, M., Holdak, A., Kokhanovsky, A., Livschitz, J. and Eisinger, M.: The GOME-2 instrument on the Metop series of satellites: instrument design, calibration, 30 and level 1 data processing – an overview, *Atmos. Meas. Tech.*, 9(3), 1279–1301, doi:10.5194/amt-9-1279-2016, 2016.
- Nakajima, T. and King, M. D.: Determination of the Optical Thickness and Effective Particle Radius of Clouds from Reflected Solar Radiation Measurements. Part I: Theory, *J. Atmos. Sci.*, 47(15), 1878–1893, doi:10.1175/1520-

- 0469(1990)047<1878:DOTOTA>2.0.CO;2, 1990.
- Natraj, V. and Spurr, R. J. D.: A fast linearized pseudo-spherical two orders of scattering model to account for polarization in vertically inhomogeneous scattering-absorbing media, *J. Quant. Spectrosc. Radiat. Transf.*, 107(2), 263–293, doi:10.1016/j.jqsrt.2007.02.011, 2007.
- 5 O'Brien, D. M. and Mitchell, R. M.: Error Estimates for Retrieval of Cloud-Top Pressure Using Absorption in the A Band of Oxygen, *J. Appl. Meteorol.*, 31(10), 1179–1192, doi:10.1175/1520-0450(1992)031<1179:EEFROC>2.0.CO;2, 1992.
- O'Dell, C. W.: Acceleration of multiple-scattering, hyperspectral radiative transfer calculations via low-streams interpolation, *J. Geophys. Res.*, 115(D10), D10206, doi:10.1029/2009JD012803, 2010.
- Osterman, G. B., Eldering, A., Avis, C., Chafin, B., O'Dell, C. W., Frankenberg, C., Fisher, B. M., Mandrake, L., Wunch, D., Granat,
- 10 R. and Crisp, D.: Orbiting Carbon Observatory-2 (OCO-2) Data Product User's Guide, Operational L1 and L2 Data Versions 7 and 7R, Pasadena, CA., 2016.
- Platnick, S. , Ackerman, S. A., King, M. D., Meyer, K. , Menzel, W. P. , Holz, R. E. , Baum, B. A. . and P., Y.: MODIS atmosphere L2 cloud product (06_L2), , doi:dx.doi.org/10.5067/MODIS/MYD06_L2.006, 2015.
- Rabier, F., Fourrié, N., Chafaï, D. and Prunet, P.: Channel selection methods for Infrared Atmospheric Sounding
- 15 Interferometer radiances, *Q. J. R. Meteorol. Soc.*, 128(581), 1011–1027, doi:10.1256/0035900021643638, 2002.
- Richardson, M., McDuffie, J., Stephens, G. L., Cronk, H. Q. and Taylor, T. E.: The OCO-2 oxygen A-band response to liquid marine cloud properties from CALIPSO and MODIS, *J. Geophys. Res. Atmos.*, doi:10.1002/2017JD026561, 2017.
- Rodgers, C. D.: *Inverse Methods for Atmospheric Sounding Theory and Practice*, World Scientific, Singapore., 2000.
- Rozanov, V. V. and Kokhanovsky, A. A.: Semianalytical cloud retrieval algorithm as applied to the cloud top altitude and the
- 20 cloud geometrical thickness determination from top-of-atmosphere reflectance measurements in the oxygen A band, *J. Geophys. Res.*, 109(D5), D05202, doi:10.1029/2003JD004104, 2004.
- Schuessler, O., Loyola Rodriguez, D. G., Doicu, A. and Spurr, R.: Information Content in the Oxygen A -Band for the Retrieval of Macrophysical Cloud Parameters, *IEEE Trans. Geosci. Remote Sens.*, 52(6), 3246–3255, doi:10.1109/TGRS.2013.2271986, 2014.
- 25 Shannon, C. and Weaver, W.: *The Mathematical Theory of Communication*, Univ. of Illinois Press, Urbana, IL, U.S.A., 1949.
- Spurr, R. J. D.: VLIDORT: A linearized pseudo-spherical vector discrete ordinate radiative transfer code for forward model and retrieval studies in multilayer multiple scattering media, *J. Quant. Spectrosc. Radiat. Transf.*, 102(2), 316–342, doi:10.1016/j.jqsrt.2006.05.005, 2006.
- Spurr, R. J. D., Kurosu, T. P. and Chance, K. V.: A linearized discrete ordinate radiative transfer model for atmospheric remote-
- 30 sensing retrieval, *J. Quant. Spectrosc. Radiat. Transf.*, 68(6), 689–735, doi:10.1016/S0022-4073(00)00055-8, 2001.
- Stephens, G. and Heidinger, A.: Molecular Line Absorption in a Scattering Atmosphere. Part I: Theory, *J. Atmos. Sci.*, 57(10), 1599–1614, doi:10.1175/1520-0469(2000)057<1599:MLAIAS>2.0.CO;2, 2000.

- Stephens, G. L.: Radiation Profiles in Extended Water Clouds. II: Parameterization Schemes, *J. Atmos. Sci.*, 35(11), 2123–2132, doi:10.1175/1520-0469(1978)035<2123:RPIEWC>2.0.CO;2, 1978.
- Stephens, G. L., Vane, D. G., Tanelli, S., Im, E., Durden, S., Rokey, M., Reinke, D., Partain, P., Mace, G. G., Austin, R., L’Ecuyer, T., Haynes, J., Lebsock, M., Suzuki, K., Waliser, D., Wu, D., Kay, J., Gettelman, A., Wang, Z. and Marchand, R.: CloudSat mission: Performance and early science after the first year of operation, *J. Geophys. Res.*, 113, D00A18, doi:10.1029/2008JD009982, 2008.
- Szczodrak, M., Austin, P. H. and Krummel, P. B.: Variability of Optical Depth and Effective Radius in Marine Stratocumulus Clouds, *J. Atmos. Sci.*, 58(19), 2912–2926, doi:10.1175/1520-0469(2001)058<2912:VOODAE>2.0.CO;2, 2001.
- Taylor, T. E., O’Dell, C. W., Frankenberg, C., Partain, P. T., Cronk, H. Q., Savtchenko, A., Nelson, R. R., Rosenthal, E. J., Chang, A. Y., Fisher, B., Osterman, G. B., Pollock, R. H., Crisp, D., Eldering, A. and Gunson, M. R.: Orbiting Carbon Observatory-2 (OCO-2) cloud screening algorithms: validation against collocated MODIS and CALIOP data, *Atmos. Meas. Tech.*, 9(3), 973–989, doi:10.5194/amt-9-973-2016, 2016.
- Vanbauce, C., Buriez, J. C., Parol, F., Bonnel, B., Sèze, G. and Couvert, P.: Apparent pressure derived from ADEOS-POLDER observations in the oxygen A-band over ocean, *Geophys. Res. Lett.*, 25(16), 3159–3162, doi:10.1029/98GL02324, 1998.
- Vaughan, M. A., Powell, K. A., Winker, D. M., Hostetler, C. A., Kuehn, R. E., Hunt, W. H., Getzewich, B. J., Young, S. A., Liu, Z. and McGill, M. J.: Fully Automated Detection of Cloud and Aerosol Layers in the CALIPSO Lidar Measurements, *J. Atmos. Ocean. Technol.*, 26(10), 2034–2050, doi:10.1175/2009JTECHA1228.1, 2009.
- Vidot, J., Bennartz, R., O’Dell, C. W., Preusker, R., Lindstrot, R. and Heidinger, A. K.: CO₂ Retrieval over Clouds from the OCO Mission: Model Simulations and Error Analysis, *J. Atmos. Ocean. Technol.*, 26(6), 1090–1104, doi:10.1175/2009JTECHA1200.1, 2009.
- Winker, D. M., Pelon, J., Coakley, J. A., Ackerman, S. A., Charlson, R. J., Colarco, P. R., Flamant, P., Fu, Q., Hoff, R. M., Kittaka, C., Kubar, T. L., Le Treut, H., McCormick, M. P., Mégie, G., Poole, L., Powell, K., Treppe, C., Vaughan, M. A. and Wielicki, B. A.: The CALIPSO Mission: A Global 3D View of Aerosols and Clouds, *Bull. Am. Meteorol. Soc.*, 91(9), 1211–1229, doi:10.1175/2010BAMS3009.1, 2010.
- Wood, R. and Hartmann, D. L.: Spatial Variability of Liquid Water Path in Marine Low Cloud: The Importance of Mesoscale Cellular Convection, *J. Clim.*, 19(9), 1748–1764, doi:10.1175/JCLI3702.1, 2006.
- Yamamoto, G. and Wark, D. Q.: Discussion of the letter by R. A. Hanel, “Determination of cloud altitude from a satellite,” *J. Geophys. Res.*, 66(10), 3596–3596, doi:10.1029/JZ066i010p03596, 1961.
- Yang, Y., Marshak, A., Mao, J., Lyapustin, A. and Herman, J.: A method of retrieving cloud top height and cloud geometrical thickness with oxygen A and B bands for the Deep Space Climate Observatory (DSCOVR) mission: Radiative transfer simulations, *J. Quant. Spectrosc. Radiat. Transf.*, 122, 141–149, doi:10.1016/j.jqsrt.2012.09.017, 2013.
- Zelinka, M. D., Klein, S. A. and Hartmann, D. L.: Computing and Partitioning Cloud Feedbacks Using Cloud Property



5 **Figure 1** Square-root of diagonal components of the covariance matrix, stacked contribution from temperature (red), humidity (blue) and effective radius (magenta). Results shown for a cloud with $\tau = 10$ and $P_{top} = 850$ hPa. Left shows the value in absolute radiance, and right as a fraction of the unperturbed radiance such that 0.03 represents an uncertainty of $\pm 3\%$.

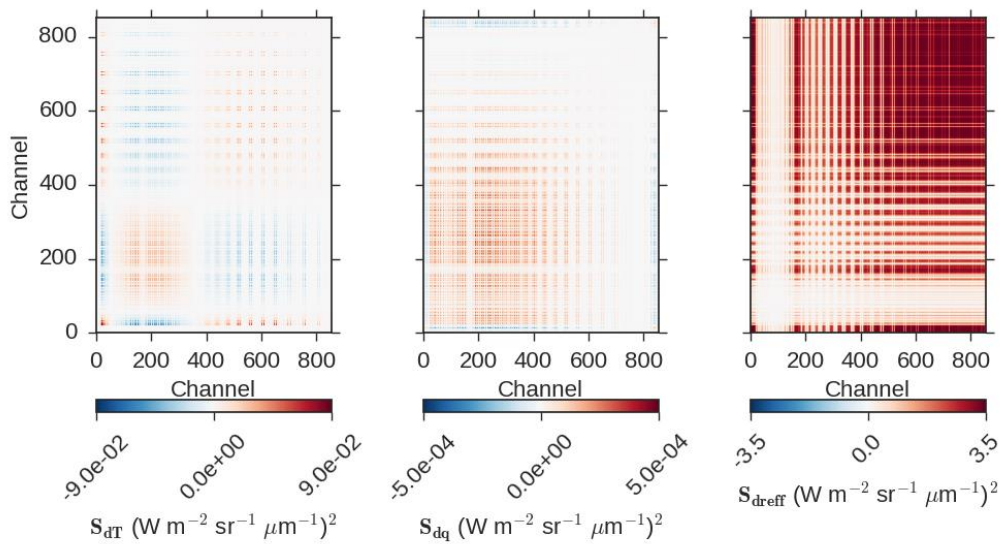


Figure 2 Example covariance matrices for each component as labelled in the colour bar: (left) temperature, (middle) humidity, (right) effective radius.

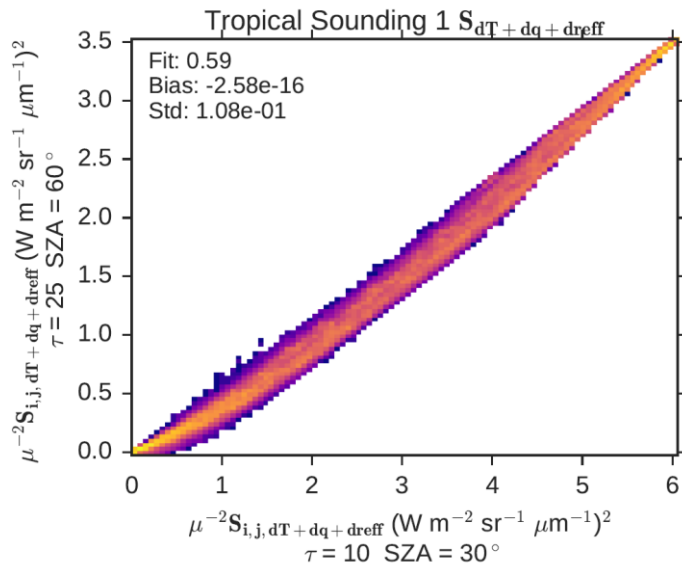


Figure 3 ~~(top)~~ 2d histograms of ~~raw~~ covariance matrix elements at 60° solar zenith angle as a function of the same values at 30° solar zenith angle for the mid-latitude meteorological state. ~~(bottom) as top, but~~ each value has been scaled by $\mu_0^{-2} = \cos^{-2}(SZA)$ to account for differences in illumination geometry.

5

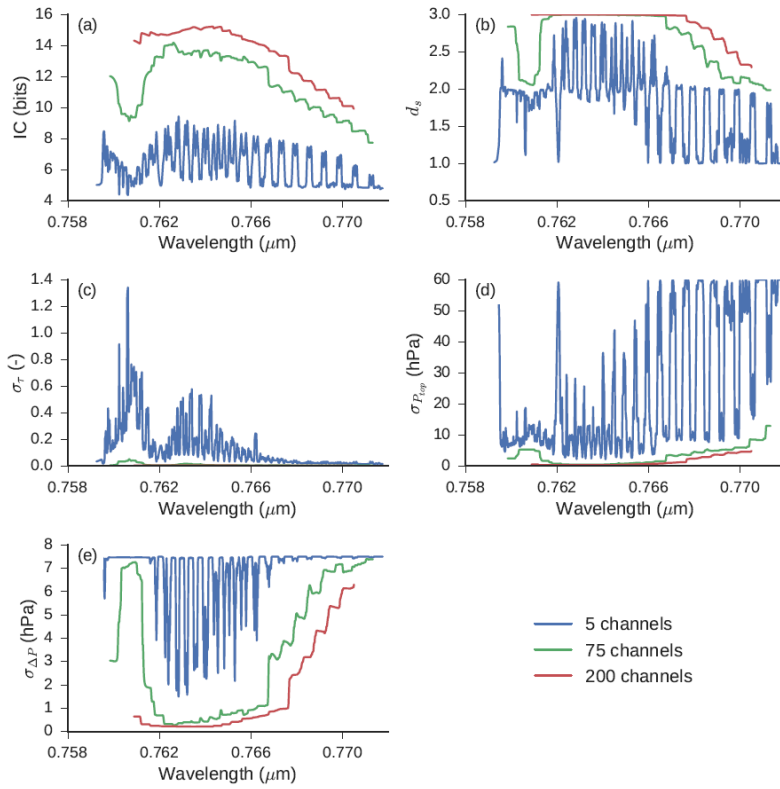


Figure 4 Results of information content analysis for a $\tau = 10$ and $P_{top} = 850$ hPa cloud in mean mid-latitude meteorology for OCO-2 sounding position 1. Each line represents the result using a micro-window of difference size, centred on the OCO-2 pixel channel given in the x-axis. Values are as follows: (a) information content in bits, (b) degrees of freedom for signal, (c)–(e) square root of diagonal elements of posterior state covariance matrix, (c) cloud optical depth, (d) cloud-top pressure and (e) cloud pressure thickness.

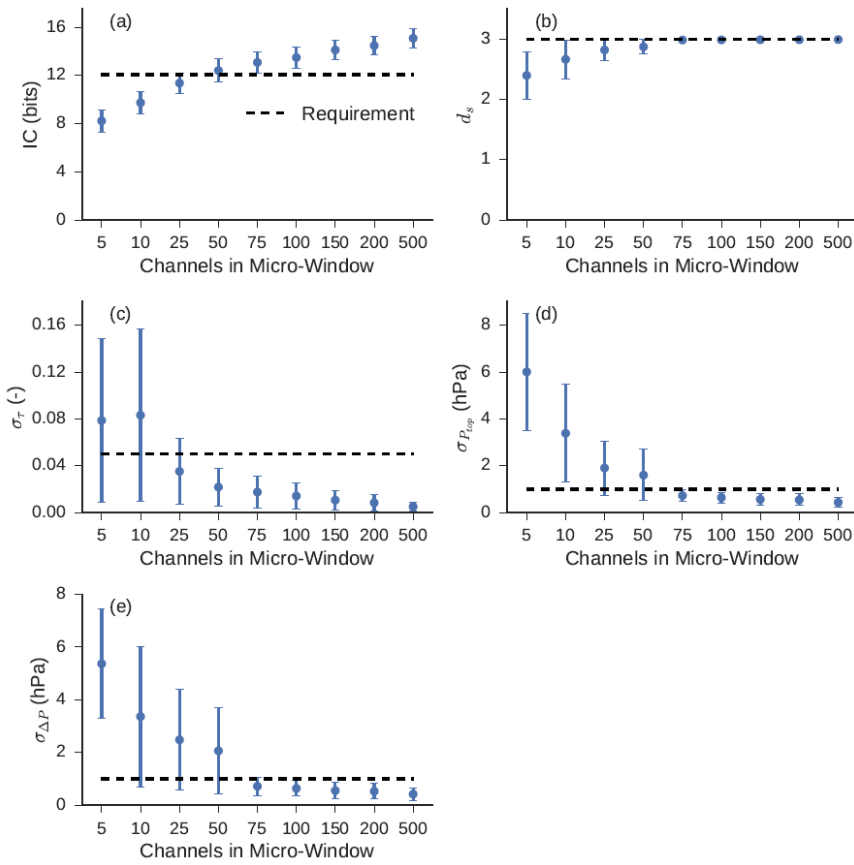


Figure 5 Range of performance for best-located micro-window of each size. The point represents the central value and the lines the full range of the 216 outputs covering each sounding position, meteorology and cloud case. Note that the x-axis is non-linear. (a) Information content in bits, (b) degrees of freedom for signal, (bc—de) square root of diagonal covariance matrix elements: (bc) cloud optical depth, (ed) cloud-top pressure and (de) cloud pressure thickness. Dashed lines represent selected retrieval requirements.

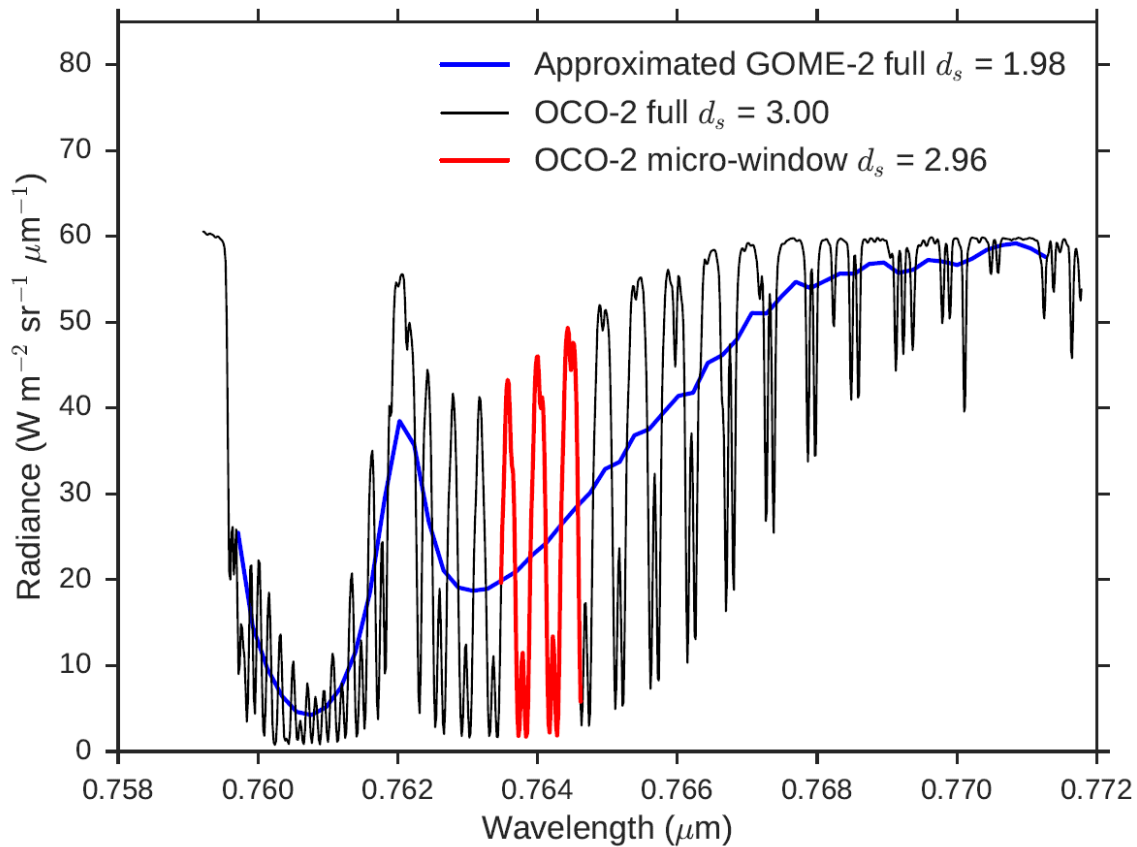


Figure 6 Example simulated cloudy scene A-band spectrum, for a $\tau = 10$, $P_{top} = 850$ hPa cloud in a tropical atmosphere with a solar zenith angle of 45° . The black line shows the full OCO-2 simulated spectrum, the blue line is the black line resampled using approximate GOME-2 instrument line shapes and the red line is the selected 75 channel micro-window for OCO-2 cloud retrievals. The legend also reports the d_s for each spectrum with the GOME-2 instrumental uncertainty based on an SNR of 100 as in previous work (Schuessler et al., 2014). Improving SNR to OCO-2-like levels also results in d_s of near 2 for the GOME-2-like spectrum.

5

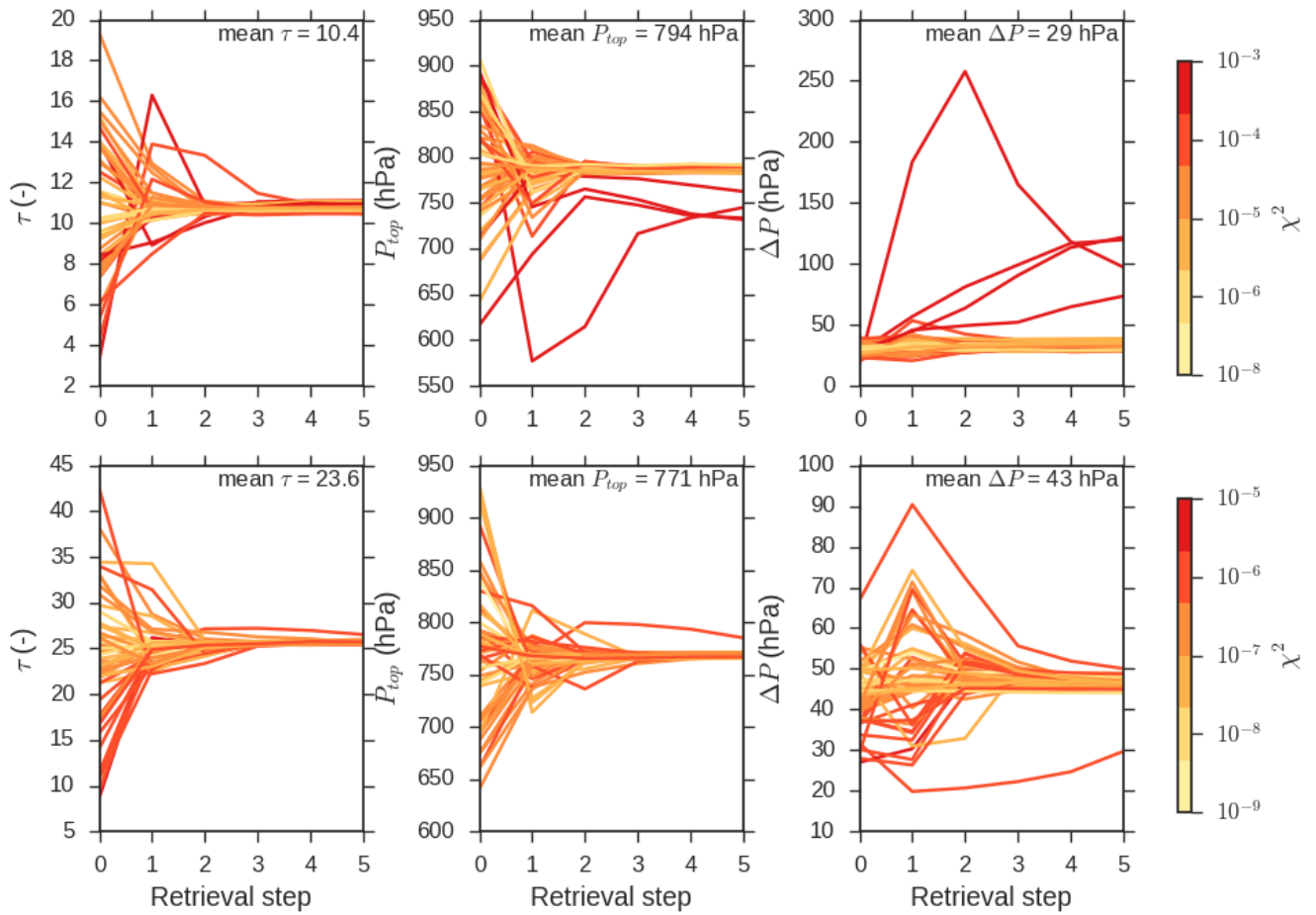


Figure 7 Example iteration in retrieved cloud properties for synthetic micro-window retrievals for test cases with cloud optical depth near 10 (top) and 25 (bottom). Each line represents the iterations through one of the 50 sample retrievals. The lines are coloured according to their χ^2 values, note the separate colour bars for the top and bottom rows with larger χ^2 for the top cases.

5

10

Table 1 – Posterior errors estimated from the sample standard deviations of the retrieval output. In each case, σ refers to the full sample standard deviation and σ (filtered) refers to the sample standard deviation excluding those with the 10 % highest values of χ^2 . The bottom row shows the mean of the standard deviations entered in each row.

True τ	τ		ctP (hPa)		dP (hPa)	
	σ	σ (filtered)	σ	σ (filtered)	σ	σ (filtered)
5	0.22	0.22	6.5	6.3	5.3	5.3
10	0.27	0.25	13.7	2.3	22.0	2.5
15	0.46	0.45	1.8	1.8	1.0	1.0
20	0.15	0.15	1.3	1.3	0.8	0.8
25	0.13	0.13	1.4	1.3	0.9	1.0
30	0.32	0.32	1.5	1.4	1.2	1.1
35	7.52	1.95	19.5	2.9	11.3	3.1
40	15.27	0.49	26.7	2.3	26.4	0.9
Average	6.02	0.75	12.9	2.9	12.9	2.5